BIOREV (2017) 6: 223–262
DOI: 10.1007/11663_2015_5001

Published online: 1 March 2016

# Recent Advances in the Study of Electrochemistry of Redox Proteins

**Preety Vatsyayan**

**Abstract** Redox proteins constitute a diverse class of proteins that facilitate the chemical and biological processes which are otherwise thermodynamically challenging. Efficient catalysis, diversity of biotransformation, potent redox centres and fast electron transport kinetics make these redox proteins an interesting target for electrochemical investigation for both theoretical and practical implications. The first and foremost requirement for electrochemical studies of redox proteins is to create an environment where they could interact with the electrodes either directly or via electron transport mediators. The last few years have seen a tremendous development in this field ranging from the increase in diversity of redox proteins that could possibly be studied electrochemically to their efficient immobilisation in a variety of matrices especially nanomatrices. Major advances have also been made in the area of characterisation of fabricated bioelectrodes by using different spectroscopic and microscopic techniques supplementing the electrochemical findings. This chapter will focus mainly on the aforementioned recent developments in the field of electrochemical studies of redox proteins and their applications for studies of redox mechanism or as biosensors or biofuel cells.

**Keywords** Biofuel cell • Biosensor • Immobilisation • Protein structure–function • Redox proteins

## Contents



P. Vatsyayan (✉)
Institute of Analytical Chemistry, Chemo- and Biosensors, University of Regensburg, 93053 Regensburg, Germany
e-mail: preety.vatsyayan@chemie.uni-regensburg.de

## Abbreviations

| | |
|---|---|
| ACNTs | Aligned carbon nanotubes |
| AFM | Atomic force microscopy |
| ArO | Arsenite oxidase |
| AuNPs/NWs | Gold nanoparticles/nanowires |
| Az | Azurin |
| CAT | Large catalase |
| cbo3 | Cytochrome bo3 |
| CcO | Cytochrome c oxidase |
| ChOx | Cholesterol oxidase |
| CV | Cyclic voltammetry |
| CYP | Cytochrome P450 |
| cyt c | Cytochrome c |
| D/ET | Direct/electron transfer |
| DDAB | Didodecyldimethylammonium bromide |
| EFCs | Enzymatic fuel cells |
| EIS | Electrochemical impedance spectroscopy |
| FAD | Flavin adenine dinucleotide |
| FT/IR | Fourier transform/infrared |
| GCE | Glassy carbon electrode |
| GOx | Glucose oxidase |
| Hb | Haemoglobin |
| HRTEM | High-resolution transmission electron microscopy |
| hSO | Human sulphite oxidase |
| $k_s/k_{ET}$ | Electron transfer rate constant |
| M/SWCNTs | Multi/single-walled carbon nanotubes |
| MP-11 | Microperoxidase-11 |
| MW | Molecular weight |
| NADH | Nicotinamide adenine dinucleotide |
| NapAB | Nitrate reductase |
| NF | Nafion® |
| PANI-NTs | Polyaniline nanotubes |
| PEI | Polyethyleneimine |

| | |
|---|---|
| PFV | Protein film voltammetry |
| PGE | Pyrolytic graphite edge |
| QCM | Quartz crystal microbalance |
| $R_{ct}$ | Charge transfer resistance |
| SAM | Self-assembled monolayer |
| SCE | Saturated calomel electrode |
| SEM | Scanning electron microscopy |
| SHE | Standard hydrogen electrode |
| SPR | Surface plasmon resonance |
| tBLMs | Tethered bilayer membranes |

## 1 Introduction

Redox proteins are a class of biological molecules responsible for many important functions in living organisms. They act as mediators for electron flow to cover the energy gap between source and sink in respiratory or photosynthetic chains, e.g. cytochromes, plastoquinones, etc. [1]. Some of them act as biological catalysts facilitating oxidation and reduction of a substrate or a group of substrates with the addition or removal of a proton ($H^+$) or electron ($e^-$). Enzymes mostly included in this class are dehydrogenases, oxidases, peroxidases, etc. which carry out reactions ranging from oxidation of glucose to detoxification of xenobiotics inside the living cells [2]. Another group of redox proteins is involved in transfer of $O_2$ inside the blood and muscles (e.g. haemoglobin and myoglobin). Thus redox proteins constitute a diverse class of proteins that facilitate the chemical and biological processes that are otherwise thermodynamically challenging. Most of these proteins contain metals especially first-row transition metals alone or in a prosthetic group as their redox-active centres, e.g. iron in cytochromes, copper in cupredoxins, zinc in nucleases and transcription factors, etc. to name a few [3]. Sometimes they require cofactors such as flavins or quinones as their redox partners, e.g. glucose oxidase (GOx) and plastoquinone, respectively. Efficient catalysis, diversity of biotransformation, potent redox centres and fast electron transport kinetics make these redox proteins an interesting target for electrochemical investigation for both theoretical and practical implications [4–7].

The first and foremost requirement for electrochemical studies of redox proteins is to create an environment where they could interact with the electrodes either directly or via electron transport mediators. This could be achieved either in solution or by confinement of proteins onto electrodes by immobilisation or wiring. Although, electrochemical studies of redox proteins in solution are relatively simple and have been practised since the 1970s [8, 9], they are mostly limited by various factors, e.g. the tendency of proteins to adsorb and denature at electrode surfaces, their diffusional limitation because of their large sizes compared to other chemical molecules in the solution, slower in and out electron flow due to the deeply buried redox centres inside the protein matrices and their dilution in solution

compared to when they are confined to electrode surfaces. Immobilisation of redox proteins for electrochemical studies is normally done to overcome the limitations faced in solution studies. The immobilisation of proteins over electrodes also paves the way towards their miniaturisation for practical applications such as biosensors or biofuel cells. The recent studies related to electrochemistry of redox proteins largely focus on their immobilisation in suitable matrices or wiring over the electrode surfaces to maintain their structural integrity and orientation for stable and efficient electron transfer [10, 11].

The field of electrochemical studies of redox proteins from its theory to application has been extensively reviewed and documented since its inception in 1970s [4–7, 12–19]. The last few years have seen a tremendous development in this field ranging from the diversity of proteins (small to large, monomeric to multimeric, cytoplasmic to membrane bound, simple to complex) that could possibly be studied electrochemically to their efficient immobilisation in a variety of matrices especially nanomatrices. Major advances have also been made in the areas of characterisation of fabricated bioelectrodes and their applications for studies of redox mechanism or as biosensors or biofuel cells. This chapter will focus mainly on the aforementioned recent developments in the field of electrochemical studies of redox proteins with a brief discussion over the theory and instrumentation required to understand the context.

## 2 Instrumentation/Theory

Electrochemical study of redox proteins starts with the selection of an electrode/transducer surface that can act as a source/sink for electrons in the redox cycle. It also provides a surface for capturing redox proteins in protein film voltammetry (PFV) or for modification by different techniques of protein immobilisation. The electrode material should be chemically inert, non-toxic to biological processes and conductive to support efficient electron transfer. The commonly used electrodes for protein electrochemical studies are either metallic (Au, Pt, Ag) or made up of carbon (graphite, glassy carbon, etc.) [12, 20]. Metal surfaces especially gold are frequently used on which a monolayer of adsorbate can easily be self-assembled (SAM). The adsorbates are usually bifunctional molecules such as $X\text{-}(CH_2)_n\text{-}Y$, where X is a substituent that anchors the molecule on the metal electrode surface (e.g. a thiol) and Y is a functional group (typically carboxyl for basic proteins like cytochrome c or amine for acidic proteins such as plastocyanin or ferredoxins) which forms amide bonds with proteins via carbodiimide coupling. Other metals such as platinum, silver and sometimes nickel are also used as electrode materials. Graphite is also among the most frequently used electrode materials on which rapid and reversible electrochemistry of redox proteins is often observed even without surface modifications. One such graphite electrode is pyrolytic graphite (PG) which is formed by the deposition of carbon from the vapour phase and has a crystalline structure. It provides two highly distinctive types of surfaces depending upon the

plane along which it is cleaved – edge or basal. Edge or basal plane PG electrodes provide surfaces for hydrophilic or hydrophobic interactions, respectively. The electrode surfaces can also be modified to provide other functional groups for protein cross-linking or adsorption.

The electrochemical experiments of redox proteins are usually carried out using an electrochemical analyser or potentiostat in conjunction with the cell. The cell consists of mainly three electrodes: reference, working and auxiliary or counter electrode. The analyser measures the current registered in response to the potential that is applied. In general, the potential of the working electrode (vs. the reference electrode) is modulated (e.g. in a linear sweep), and the current between the working electrode and the counter electrode is recorded. It is the working electrode where the redox protein is immobilised and/or its redox properties are studied.

*Cyclic voltammetry* (*CV*) is the most popular method for studying redox protein electrochemistry. The electrode potential is swept forward and backward with a scan rate (in units of V $s^{-1}$), and a voltammogram is generated which is a plot of current against electrode potential. CV is extensively used to evaluate the electron transfer properties of redox proteins for their thermodynamic, kinetic and mechanistic information. Ideally at slow scan rates for thin film of proteins over the electrode, the CVs are predicted to have symmetric oxidation and reduction peaks with both peak potentials at the formal potential ($E^{\circ\prime}$), and the oxidation–reduction peak separation ($\Delta E_p$) equals to zero. The surface coverage ($\Gamma$) of redox protein over the electrode is described by the equation, $\Gamma = Q/nFA$, where $Q$ is charge obtained by integrating the peak current area, $n$ is number of electrons transferred, $F$ is Faraday's constant and $A$ is the electrode area. When the ideal thin-layer protein film model is followed, results of $\Delta E_p$ vs. scan rate can be used to estimate the surface electron transfer rate constant $k_s$ ($s^{-1}$) [16, 20, 21].

*Electrochemical impedance spectroscopy* (*EIS*) is a valuable tool for characterising surface modifications during immobilisation of biomolecules over the transducer surface [22]. The biological component is generally immobilised on the working electrode with layer/s of immobilisation matrix. This alters the resistive or capacitive properties of the electrode. For EIS studies, a low-amplitude *AC* potential is applied through the cell, and the interaction of modified electrode with a redox analyte in the solution is measured over a wide range of frequencies to generate an impedance spectrum. The data can be plotted in different forms such as Nyquist plot, Cole–Cole plot, etc. The immobilisation layers over the working electrode result in a well-defined charge transfer resistance $R_{ct}$ or impedance $Z$, e.g. a blocking layer will cause increase in $R_{ct}$ and vice versa.

*Catalytic protein voltammetry and chronoamperometry* are generally used to characterise the electrochemical activity of redox proteins [16, 20]. In the absence of substrate and at sufficiently high surface coverage, a redox protein immobilised onto an electrode gives peak-like signals resulting from the reversible transformation of its redox centres. However, upon addition of substrate, the non-turnover peaks are transformed to sizeable catalytic waves. Reaction with substrate transforms the active site, which is regenerated by electron exchange with the electrode in a succession of catalytic cycles. The magnitude of the current is proportional to

electroactive coverage and to turnover rate, and so the relationship between potential and catalytic activity is traced in a single voltammetric experiment. Alternatively, in an experiment called chronoamperometry, the electrode potential is held at a fixed value, and the current is recorded as a function of time with increasing/decreasing substrate/inhibitor concentrations.

Besides above-mentioned classical electrochemical techniques, many other microscopic and spectroscopic techniques are routinely used for bioelectrode characterisation which help to fortify the electrochemical findings. Microscopic techniques especially atomic force microscopy (AFM), scanning electron microscopy (SEM), transmission electron microscopy (TEM), etc. are largely used to image surface topography of electrodes after immobilisation of redox proteins in different matrices [23–25]. Electronic absorption spectroscopy has been used for long time to study redox protein interactions with immobilisation matrices [26, 27]. Recently different forms of vibrational spectroscopy such as infrared (IR), Raman, etc. are used frequently to characterise immobilisation matrices and to study their interactions with redox proteins [25, 26]. With the onset of the use of nanomaterials such as gold nanoparticles (AuNPs), it is now possible to characterise the AuNP-modified redox proteins or electrodes with surface plasmon resonance (SPR) [28]. Gravimetric technique like quartz crystal microbalance (QCM) is used to calculate the surface coverage of immobilised redox proteins over the electrode by measuring the change in frequency of crystal [24]. Elaborating on the principles of all these techniques is out of context for this chapter, but their usages for bioelectrode characterisation or as supporting evidence for electrochemical studies have been included wherever applicable in the following sections.

## 3 Immobilisation of Redox Proteins

Proteins being biological macromolecules are highly sensitive to rapid denaturation once isolated from the natural environment/living cells and have a small shelf life in solution at room temperature. The effect of immobilisation on improvement of enzyme activity, stability and selectivity has long been established for industrial applications and has been reviewed [29]. For electrochemical studies also immobilisation of redox proteins over electrode surfaces helps to overcome many of the limitations faced in solution studies. Many a times, immobilising a redox protein on an electrode is the only way to study them electrochemically. Besides, immobilisation of proteins also enhances the probability of electrodes to act as their redox partners for direct electron transfer (DET) which helps in better understanding of protein electrochemistry. Although, it adds additional steps to find suitable matrices and to develop strategies for immobilisation of different proteins that provide maximum stability and efficiency over the electrode surfaces, the benefits achieved later make it worth pursuing. Most of the immobilisation techniques discussed here facilitate direct electron transfer between redox proteins and electrodes.

### 3.1 To Mimic the Natural Environment

Immobilisation of proteins in suitable matrices sometimes mimics their natural environment and enhances their structural and functional stability. Membrane-associated proteins form a large class of redox proteins and are frequently involved in respiratory electron transport chains and photosystems besides other functions in living cells. They are usually large in size with hydrophobic patches and tend to lose their structural integrity and activity once brought into the solution [30]. As a result, the electrochemical studies with membrane proteins especially integral membrane proteins have made significantly less progress compared to globular proteins.

*Lipid films* are widely used to mimic the bilayer structure of membrane over the electrodes for immobilisation of membrane-associated redox proteins. They impart structural stability and also preserve the conformational freedom of macromolecules for their function [31, 32]. Besides, lipid films also protect the solid support from undesirable interferences and thus minimise redox processes at the electrode surface. The power of lipid films was realised long back when a reversible electrochemistry for cytochrome P450cam was observed for a month with only 10% decrease in activity after immobilisation in dimyristoylphosphatidylcholine (DMPC) films [33]. In solution the activity degraded completely in less than a day. The redox proteins can be incorporated into the lipid films either by dissolution of the protein molecules in the lipid solution from which the film is prepared or by immobilisation of the protein on the lipid film surface.

A recent review by Khan et al. [34] provides detailed insight into the engineering of lipid bilayers over different electrode materials for protein immobilisation and their electrochemical studies. Jeuken [31] summarised different strategies for bilayer assembly over metal (gold and silver) or graphite electrodes for electrochemical studies of cytochrome c oxidase (CcO), a representative protein for integral membrane-bound proteins. CcO was incorporated either into a hybrid bilayer membrane (consisting of SAM of alkane thiols over a metal electrode and a phospholipid monolayer) or in a pure phospholipid bilayer. The pure phospholipid bilayer was either directly adsorbed on the electrode or tethered to the electrode surface with lipid thiols (tethered bilayer membranes, tBLMs). In another approach, histidine-tagged CcO was tethered to the electrode by Ni–nitrilotriacetic acid (thiol modified) affinity system, and then the phospholipid bilayer was reconstituted around the tethered protein. In hybrid bilayer and directly adsorbed lipid bilayer, the thin water layer between electrode and bilayer was not sufficient to prevent direct interaction of transmembrane proteins with electrode surface resulting in their direct adsorption at the electrode and denaturation [34]. In case of tBLMs, the space between the electrode and the lower leaflet of lipid bilayer was used for the incorporation of a hydrophilic spacer. The spacer in turn avoided the direct interaction of proteins with the electrode surface and their subsequent denaturation.

The tBLM approach was successfully used to immobilise cytochrome bo3 (cbo3), a ubiquinol oxidase from *Escherichia coli* [35]. The tBLM was formed on gold surface functionalised with cholesterol tethers which inserted itself into the

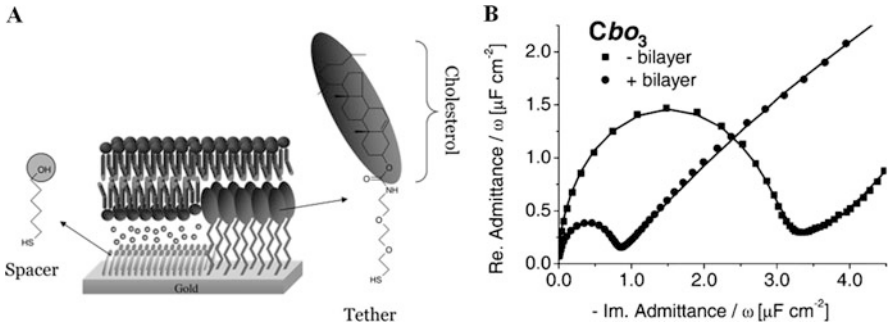


**Fig. 1** (**A**) Schematic representation of a tBLM formed on a mixed self-assembled monolayer of tether (cholesterol) and spacer molecules (6-mercaptohexanol). (**B**) Cole–Cole plots for cbo3 before and after formation of a tBLM measured at 0 V vs. SCE. Adapted with permission from [35]. Copyright (2006) American Chemical Society

lower leaflet of the membrane (Fig. 1A). 6-Mercaptohexanol was used as the hydrophilic spacer. The planar membrane architecture was formed by self-assembly of proteoliposomes, and its structure was characterised electrochemically by EIS. Normally, the double-layer capacitance of an ideal phospholipid bilayer should be around 0.5 μF $cm^{-2}$. A drastic increase in the capacitance is generally caused by some disorder or defect in the bilayer. Incorporation of a protein also increases the capacitance values, as a result of the higher dielectric constant and disorder in the bilayer. As shown in Fig. 1B, the double-layer capacitance of the tBLMs on gold electrode was around 0.7–0.8 μF $cm^{-2}$ which was only slightly larger than that of the ideal and was almost the same both in the absence (figure not shown) and presence of cbo3. These results showed that the inclusion of cbo3 had almost no effect on the double-layer capacitance of the tethered membrane and did not induce large defects in the tethered bilayer. The functionality of tBLM-immobilised cbo3 was investigated by CV and was confirmed by catalytic reduction of $O_2$.

*Surfactant cast films* are also one of the frequently used immobilisation techniques for membrane-bound redox proteins. Surfactants are surface-active agents with a charged or polar head group and a nonpolar tail similar to naturally occurring lipids. Stable films can be cast from surfactants that are insoluble in water and do not form micelles. Molecules fulfilling these requirements have ionic or zwitterionic head groups and two or more hydrocarbon tails of 12 carbons or longer, e.g. didodecyldimethylammonium bromide (DDAB), dihexadecylphosphate (DHP), sodium dodecyl sulphate (SDS), etc. Similar to the incorporation of protein in lipid films, the redox protein is either taken up by the surfactant film already casted on the electrode or a mixture of protein and surfactant is co-casted on the electrode.

The discussion over electrochemical studies of membrane-bound redox proteins is incomplete without a mention of cytochrome P450 (CYP). CYP is one of the most important redox proteins which needs to be studied electrochemically for both

theoretical and practical applications. It is a class of monooxygenase enzymes which are used for synthesis of industrially important compounds as well as for detoxification of drugs and xenobiotics [36]. Thus it has both industrial and pharmaceutical applications. However, multiple attempts to replicate this enzyme system in vitro have been only marginally successful owing to the structural instability of CYP after membrane solubilisation and the intricate electron transfer machinery required for its catalysis. Although, the electrochemical methods are perhaps the simplest way of providing reducing equivalents to the catalytic cycle of CYP [37], the immobilisation of CYP over electrodes to retain its functional activity still remains tricky. Udit et al. [26] reported electrochemical measurements of CYP BM3 (from *Bacillus megaterium*) in DDAB surfactant films on basal plane graphite electrodes. At slow scan rates, a well-defined, chemically reversible redox couple centred at −260 mV (vs. saturated calomel electrode, SCE) was observed. This redox couple was assigned to the heme $Fe^{III/II}$ process. Thus, DDAB films facilitate electronic coupling between heme proteins and electrodes for direct electrochemistry. However, electrode-driven oxidative substrate catalysis was not observed, possibly due to conversion of P450 into P420 like structures in DDAB films. Recently, the same group used DDAB films for the electrochemical studies of full-length mammalian microsomal CYP 2B4 [27]. The studies of CYP BM3 and CYP 2B4 provide a great insight into understanding the redox behaviour of heme proteins inside the DDAB films.

### *3.2 To Impart Operational Stability*

The shelf life of proteins in solution is short as their stability is affected by various factors once they are isolated from the living cell. The major factors affecting protein stability in solution are aeration, pH, ionic strength, temperature, proteolysis or denaturation by exposure of protein to unsterile surfaces, etc. During electrochemical studies the protein in solution is exposed to many such physical and chemical denaturants. These factors cause rapid denaturation of proteins in solution and their reusability is further limited. It has been shown by many researchers that immobilisation of proteins in suitable matrices over electrodes reduces such effects and contributes towards the stability of proteins and their reusability [29].

*Mesoporous or macroporous matrices* often provide a suitable environment for immobilisation of proteins over electrodes. They are highly ordered porous thin films coated over the electrodes with pore sizes ranging from micrometres (macroporous) to few nanometres (mesoporous) where protein could either be adsorbed or cross-linked. Immobilisation of redox proteins into these pores provides them with much desired mechanical stability besides hindering their direct interaction with some of the physical denaturants such as gas bubbles, unsterile surfaces, etc. One of the important characteristics of porous materials is their high surface area/volume ratio that provides more loading space for proteins compared to flat electrode surfaces. Large surface area also favours the interaction with

external reagents. Electrically conducting porous materials (metals, carbon) contribute to increase the electroactive surface by several orders of magnitude thereby increasing the sensitivity of the resulting device. Semiconducting or non-conducting materials, such as metal oxides or organically modified ceramics or silica, are also attractive, especially in combining the mechanical stability of a rigid inorganic matrix with desired chemical reactivity.

Different strategies are used to generate such organised porous films on electrode surfaces. One strategy involves the use of nanomaterials as the building blocks and their self-assembly over electrodes. The other strategy is the generation of continuous nanostructured phases by a template route. Walcarius and Kuhn [38] reviewed the strategies involved in the generation of highly ordered mesoporous and macroporous thin films via template formation. The templates for the deposition of these films are made up of silica, latex or surfactants. Silica or latex templates over electrodes are formed either by self-assembly after evaporation of solvents or by dipping them in the solution so that a film could form over time. A derivative of Langmuir–Blodgett technique is also used where the micelles are first formed at the air–water interface of solution which are then transferred onto the electrodes. Once formed they are filled with conducting materials like carbon, metal or polymers by electrodeposition or electropolymerisation. The templates are later dissolved by HF or organic solvents to leave highly ordered, interconnected mesoporous or macroporous films over the electrodes where the redox proteins are then immobilised. Surfactant templates are generally prepared by sol–gel method where the metal, metal oxide or silica precursors are dissolved in surfactant–solvent mixture and are then deposited on the electrode either by evaporation (evaporation-induced self-assembly, EISA) or by electrodeposition (electro-assisted self-assembly, EASA) to produce mesoporous thin films.

For biological applications requiring protein immobilisation, macroporous structures are favoured as they correlate well with the protein dimensions. Proteins could be easily immobilised over the walls of the pores and would not block the connections and thus the flow of analytes and reagents. However, in mesoporous structures which have few nm pore dimensions, the immobilisation of proteins (which are usually bigger than the size of these pores or interconnections) would clog them causing the obstruction for the analyte flow and conductivity. Szamocki et al. [23] used macroporous gold electrodes for immobilisation of GOx and glucose dehydrogenase (GDH) for glucose sensing. The silica templates were built by Langmuir–Blodgett technique on flat cysteamine-modified gold electrodes. After electrodeposition of gold, the silica template was dissolved by 5% HF. The enzymes were then immobilised into the pores of the macroporous gold electrode either by glutaraldehyde cross-linking or by incorporation in an electrodeposition paint. Figure 2A and B shows the hexagonal arrangement of pores in the macroporous gold electrode. For the modification with biomolecules, especially proteins, it is very important that the interconnections between the pores are big enough to allow the large molecules to enter the pores where they can be immobilised. Earlier experiments with CV of similar substrate showed that the active surface area is highly increased compared to the geometrical surface area of

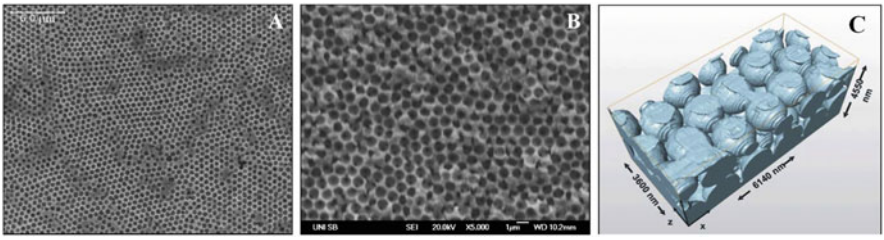


**Fig. 2** (**A**) SEM image of a macroporous electrode (*top view*) with a pore diameter of 680 nm and a thickness of the porous gold of 3½ pore layers. (**B**) Magnification of the locally ordered domains. (**C**) FIB tomography of a macroporous electrode with a diameter of 1,100 nm and a thickness of the porous gold of 1½ pore layers. The 3D image has been obtained by the reconstruction of the air-filled zones in a series of SEM images cut by a focussed ion beam every 50 nm. The substrate oriented view is shown. Adapted with permission from [23]. Copyright (2007) Elsevier

the electrode [39]. Although this provided an indirect evidence for the interconnections, to establish this fact directly and to characterise the pore dimensions, focused ion beam tomography (FIB) was used. A real 3D structure (Fig. 2C) was obtained by the reconstruction of the structure from a series of SEM images of slices cut by a focused ion beam. The figure clearly shows that every pore is connected to the neighbouring pores. From this reconstruction, it was possible to quantitatively determine the distribution of diameters of the pores and their interconnections. For a macroporous electrode with a pore diameter of 1,100 nm, the average diameter of interconnection was about 300 nm with a minimum of 200 nm. Since enzymes have a typical diameter of 20 nm, these interconnections were large enough to allow a good penetration of the enzyme and the entire internal surface to be electrochemically active.

In the same work, the effect of pore layers on sensitivity of glucose detection was also established. It was shown that for electrodes with a higher number of pore layers, thus with higher active surface area but equal geometrical area, the signal for any glucose concentration was higher. This led to higher saturation current for the electrode that could easily be increased by two orders of magnitude. This behaviour was based on the fact that on a porous electrode more glucose receptors per square centimetres were available and therefore saturation was reached only at higher concentrations. The signal difference for concentration steps in the low concentration region was higher for electrodes with a higher number of pore layers, and thus the sensitivity and the lower detection limit were also improved. When compared to a flat electrode, for an electrode with 5½ pore layers, the saturation current increased from 2.42 to 46.5 μA, the apparent Michaelis–Menten constant increased from 4.9 to 9.4 mM and the sensitivity increased from 107 μA $mol^{-1}$ $cm^{-2}$ to 1.85 mA $mol^{-1}$ $cm^{-2}$. The so prepared glucose sensors also showed a higher storage and operational stability when compared to the flat electrodes. The signal for glucose sensing was observed for a month with a gradual decrease of around 30% over a period of 7 days when stored at 4°C in Tris buffer.

In another work, a direct electron transfer of haemoglobin (Hb) was achieved by adsorbing the protein in the pores of a similarly synthesised highly ordered macroporous gold electrode prepared via silica template [40]. Its interconnected macroporous structure, containing AuNPs, significantly enhanced the amount of adsorbed Hb molecules at the monolayer level with an observed surface coverage of 88.1%. The uniform, three-dimensional macroporous gold also provided superior conductivity and higher stability to protein by providing a good microenvironment for retaining the biological activity of the adsorbed protein.

*Ionic polymer films* are one of the frequently used matrices for immobilisation of redox proteins over the electrodes. The ionic interactions of polymer films with proteins and electrodes stabilise the protein inside the matrix over the electrode surface, thereby increasing the operational stability of the resulting device. Such ionic interactions facilitate direct electron transfer between protein and electrode and also their interaction with reaction analytes. Some of the ionic polymers used for film formation are polyethyleneimine (PEI), polydiallyldimethylamine (PDDA), polystyrene sulphonate (PSS), etc. Stable polyionic polymer-protein films are constructed by the layer-by-layer electrostatic adsorption method [41]. The layer-by-layer method involves alternately adsorbing ionic macromolecules of different charges onto a surface, so that at each adsorption step, the outer layer has excess charge density enabling subsequent adsorption of a new layer of the opposite charge, thereby stabilising the whole matrix ionically. Most enzymes in these films retain high activity. This method is general and versatile and allows the film architecture to be controlled according to desired specifications. Most of the earlier electrochemical experiments with redox proteins used cytochrome c (cyt c, molecular weight, MW ~12 kDa) or other small-sized proteins as their model compounds because of their ease of handling and possibility for DET with the electrode. Electrochemical studies with bulky proteins with deeply buried redox centres were consciously avoided for their anticipated inability to interact directly with the electrodes. However, with the onset of development of various efficient immobilisation techniques lately, it is now possible to successfully study the electrochemistry of such bulky proteins too. In one such attempt, layer-by-layer electrostatic assembly technique was used for the immobilisation of large catalase (CAT, subunit MW ~90 kDa), a bulky tetrameric heme enzyme isolated and purified from *Aspergillus terreus* MTCC 6324 [42]. Figure 3A shows a schematic representation of the steps involved in the assembly of the bioelectrode, where CAT was adsorbed over multi-walled carbon nanotube/Nafion® (MWCNT/NF) nanocomposite coated on a glassy carbon electrode (GCE). Polycationic polymer PEI was used to encapsulate the assembly. The resulting bioelectrode was characterised by EIS (Fig. 3B). The spectra were presented in the form of Nyquist plots (where $Z_{re}$ is the real and $Z_{im}$ is the imaginary part of impedance) and were overlaid to pinpoint the differences in $R_{ct}$ with subsequent modification layers. Interestingly, the addition of PEI layer decreased the overall $R_{ct}$ of GCE/MWCNTs-NF/CAT assembly from about 500 to 280 Ω. As shown in the scheme (Fig. 3A), the PEI layer neutralised the negative charge density developed by the composite MWCNTs-NF/CAT (pI 4.2) and thereby reduced the charge repulsion between

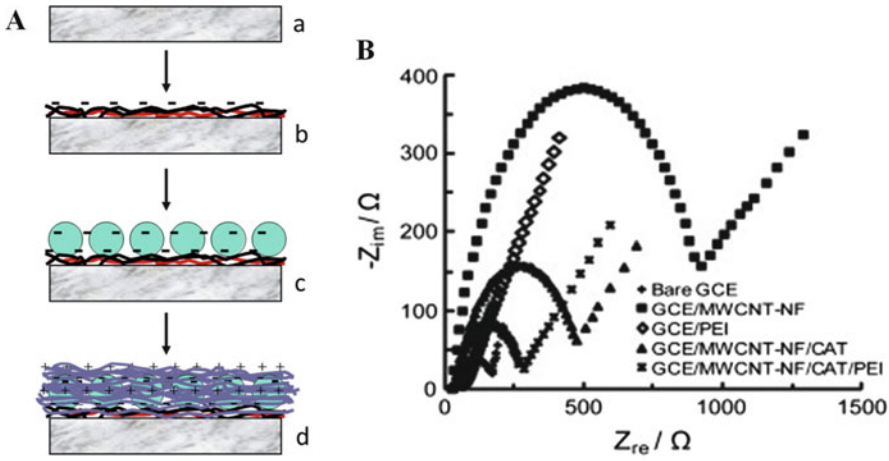


**Fig. 3** (**A**) Schematic representation (*a*) bare GCE, (*b*) GCE/MWCNT-NF, (*c*) GCE/MWCNTs-NF/CAT and (*d*) GCE/MWCNTs-NF/CAT/PEI and (**B**) EIS for layer-by-layer fabrication of CAT bioelectrode. Adapted with permission from [42]. Copyright (2010) Elsevier

the negatively charged NF and CAT resulting in decrease of the overall $R_{ct}$ of the bioelectrode. The ionic interactions of PEI layer also facilitated the direct electron transfer between the enzyme and the electrode as shown by CV experiments (not shown here). A pair of nearly reversible CV peaks for $Fe^{III/II}$ couple with $E^{\circ\prime}$ of about −0.45 V (vs. Ag/AgCl electrode at pH 7.5) was obtained for the CAT. In the same work, the effect of encapsulating layer of PEI on the stability of CAT bioelectrode was also accessed. A considerably high storage and operational stability were recorded for PEI-coated bioelectrode. The CAT activity was completely lost within 48 h without PEI compared to 75% of residual activity when encapsulated with PEI. The ionic interactions and encapsulation provided by PEI stabilised the charge density on enzyme nanocomposite assembly and prohibited the leaching of surface-bound enzyme in solution.

### *3.3 To Enhance the Electron Transfer Efficiency*

Most of the redox proteins have their active centre deeply buried inside the protein matrix which slows down or sometimes insulates the transfer of electrons from protein to the electrode. As per the classical Marcus theory for the monolayer redox couple [Eq. (1)] [16, 43, 44], $k_{ET}$ decreases exponentially with the distance of electron transfer, $d$, where $k_0$ is the electron transfer rate constant at the distance of closest contact $d_0$:

$$k_{ET} = k_0 \exp[\beta(d - d_0)] \quad (1)$$

Since, in redox protein electrochemistry, electrode and the protein redox centre are usually considered as a donor–acceptor pair, the distance or spatial separation of the protein redox centre from the electrode by means of the protein shell prohibits the direct electrical communication between the redox site and the electrode.

*Mediated electrochemistry by wiring of redox proteins* to electrodes via soluble mediators, redox metallopolymer hydrogels or conducting polymers are extensively used to overcome electron transfer barrier between redox proteins and electrodes. Mediators which could diffuse inside the protein matrix such as ferrocene derivatives, quinones, synthetic or semi-synthetic cofactors (NADH, microperoxidases, etc.), organic salts and metal bipyridine complexes have been used to shuttle electrons from proteins to electrodes [9]. Redox metallopolymers are also used as electron bridges between electrodes and redox centres of enzymes. The redox polymers are usually soluble in water and contain hydrophobic, charged or hydrogen-bonding domains, so that they can form complex with the protein and penetrate deeply into the buried redox cofactor centre to facilitate electron transfer. In addition, the polymers are also able to achieve a three-dimensional network that allows rapid diffusion of the substrate and fast charge transport. $Os^{III/II}$ redox hydrogels such as poly(vinylpyridine)-[bis(2,2′-bipyridine)chloroosmium]$^{+/2+}$, poly(vinylimidazole) complex of [bis(2,2′-bipyridine)chloroosmium]$^{+/2+}$, polyvinyl imidazole complex of [(Os-4,4-dimethyl-2,2-bipyridine)Cl]$^{2+/+}$, poly (allylamine) with attached ferrocene (PAA–Fc), poly(*N*-isopropylacrylamide-co-vinylferrocene) polymer, etc. were used extensively to mediate GOx and peroxidase electrochemistry [16, 41]. In one of the recent studies, Plumeré et al. [45] immobilised an $O_2$-sensitive hydrogenase in the viologen-functionalised redox hydrogel film on the electrode surface. Under pure $H_2$ atmosphere, the polymer/hydrogenase-modified electrodes displayed stable catalytic currents. The catalytic wave for $H_2$ oxidation was centred on viologen redox couple ($E_{V++/V+\bullet} = -0.3$ V vs. standard hydrogen electrode, SHE), demonstrating that the viologen moieties were exclusively responsible for ET from the hydrogenase to the electrode. Interestingly, the integration of the $O_2$-sensitive hydrogenase into the viologen-based redox polymer film also protected the enzyme from $O_2$ damage and high-potential deactivation thereby increasing the operational stability of the enzyme. Electron transfer between the polymer-bound viologen moieties controlled the potential applied to the active site of the hydrogenase and thus insulated the enzyme from excessive oxidative stress. Under catalytic turnover, electrons provided from the $H_2$ oxidation reaction induced viologen-catalysed $O_2$ reduction at the polymer surface, thus providing self-activated protection from $O_2$. The advantages of this tandem protection were demonstrated using a single-compartment biofuel cell based on an $O_2$-sensitive hydrogenase anode and $H_2/O_2$ mixed feed. Conductive polymers such as polypyrrole (PPy), polyaniline (PANI), polythiophene and polyindole are also used to wire redox proteins to the electrodes for their electrochemical studies. They can be grown on electrode surfaces by electrochemical polymerisation. Film

thickness can be controlled by the amount of charge consumed during electropolymerisation. The resulting polymers sometimes also exhibit low interference in sensor applications resulting from size exclusion. Redox proteins can be entrapped into the polymer network during electropolymerisation. The high inherent electron conductivity of these polymers has fostered their use as molecular wires to shuttle electrons between the redox-active sites of the proteins and electrodes. Recently many authors have extensively reviewed the use of conducting polymers for electrochemical studies of redox proteins directed towards their biosensing applications [46–48]. Although the different mediators discussed so far have been successful in establishing ET communication between the redox centres and electrodes, the bioelectrocatalytic features of the resulting enzyme electrodes represent the collective properties of numerous configurations of enzyme molecules of variable degrees of loading with electron mediator groups that reach a variety of orientations in respect to the conductive support. These difficulties limit the ET communication of the biocatalysts and the conductive supports, as compared to the ET efficiency between the enzyme redox sites and their natural ET substrates or cofactors. Besides, mediated electrochemistry suffers from its own limitations where the electrochemistry of mediators usually predominates and provides only indirect information about the protein electrochemistry or its electrocatalytic activity.

*Reconstitution of redox proteins* over their natural cofactors wired to the electrode via different approaches provides an interesting alternative for enhancing the electron transfer efficiency between redox proteins and electrodes. Willner and co-workers [17, 49] have extensively worked and reviewed this approach for both the fundamental understanding of electron transfer and their applications for biosensor and biofuel cell. The reconstitution method involves the exclusion of the native active centre from the protein, for example, an ion or a cofactor, to yield the respective apoprotein (or hollow protein). The redox-active ion or cofactor is then wired on the electrode. The reconstitution of apoprotein around wired cofactors allows the direct electrical contact of protein to the electrode. A volume of work has been done mainly with GOx and iron-containing proteins by first removing their flavin adenine dinucleotide (FAD) cofactor or heme prosthetic group, respectively, and then wiring them to the electrode via a molecular relay, conducting polymer or some nanotechnological means and reconstituting the apoprotein around them.

In one of the representative work, Patolsky et al. [24] demonstrated the reconstitution of apo-GOx on FAD cofactor electrically contacted to the electrode via single-walled carbon nanotubes (SWCNTs), which act as conductive nanoneedles that electrically wire the enzyme redox-active site to the transducer surface (Fig. 4A). Before immobilisation, the commercially obtained SWCNTs were chemically shortened by treatment with strong acids. The formation of carboxylic (and phenolic) groups at the nanotube ends (and sidewall defect sites) as a result of acid treatment allowed the covalent immobilisation of the SWCNTs on thioethanol/cysteamine-modified Au electrode in the presence of the coupling reagent 1-ethyl-3-(3-dimethylaminopropyl)carbodiimide hydrochloride (EDC) as depicted in Fig. 4A. The incorporation of 2-thioethanol in the mixed monolayer prevented

the nonspecific (as well as horizontal) adsorption of the surfactant-protected SWCNTs onto the electrode surface. The amino derivatives of the FAD cofactor were then coupled to the carboxyl groups at the free edges of the standing SWCNTs (after wall protection in the presence of surfactants Triton X-100 and PEG, MW = 10,000). Apo-GOx was then reconstituted on the FAD units linked to the ends of the standing SWCNTs. The pretreatment of the SWCNT monolayer with a mixture of the surfactants prior to the binding of FAD units and reconstitution with apo-GOx was found to be an essential step to generate a bioelectrocatalytically active interface, with the enzyme specifically coupled to the SWCNTs' FAD-modified ends. The reconstitution of the apo-GOx units on the FAD units linked to the ends of the SWCNTs was supported by AFM measurements (Fig. 4B). Figure 4C shows the high-resolution TEM image (HRTEM) of a SWCNT modified with two GOx units (negatively stained with uranyl acetate) at the edges of the tube. Voltammetric experiments revealed that FAD units were electrically connected with the electrode surface with a quasi-reversible CV ($E^{\circ\prime} = -0.45$ V vs. SCE at pH 7.4). The bioelectrocatalytic oxidation of glucose was observed at $E > 0.18$ V vs. SCE, and the electrocatalytic anodic current increased with increasing concentrations of glucose with a saturation at 60 μA. The modification of the electrode surface with the reconstituted GOx units was further characterised by means of microgravimetric QCM and electrochemical experiments. From the frequency changes of the crystals in QCM and the CVs of the FAD units, the surface coverage of the SWCNTs and of the GOx units were calculated to be $4 \times 10^{-11}$ mol cm$^{-2}$ (3–4 FAD units per SWCNT) and $1 \times 10^{-12}$ mol cm$^{-2}$, respectively. Thus, the turnover rate of 4,100 s$^{-1}$ was calculated for electrons transferred from reconstituted GOx to the electrodes. This value is about six fold higher than the turnover rate of electrons from the active site of GOx to its natural $O_2$ electron acceptor (700 s$^{-1}$) proving the enhanced electrocatalytic efficiency of reconstituted GOx after wiring of FAD to the electrode.

The electron pumping from reconstituted GOx to the electrode via FAD wiring was further established in another work by Lioubashevski et al. [28]. Apo-GOx was reconstituted on FAD cofactor-functionalised AuNPs (1.4 nm) linked to the bulk Au electrode via dithiol monolayer. Although the reconstituted GOx/AuNP hybrid system exhibited electrical communication between the enzyme redox cofactor and the AuNPs [50], an overpotential (0.4 V) was recorded for bioelectrocatalytic oxidation of glucose by the hybrid system. This positive potential shift was attributed to the tunnelling barrier introduced by the dithiolate spacer that bridged the AuNPs to the bulk electrode. To establish this observation, the GOx/AuNP hybrid was linked to the bulk Au electrode by a short dithiol, 1,4-benzenedithiol, or a long dithiol, 1,9-nonanedithiol, monolayer. Because the thiol monolayers provided a barrier for electron tunnelling, the electron transfer occurring upon the biocatalytic oxidation of glucose resulted in AuNPs charging. The charging of AuNPs altered the plasma frequency and dielectric constant of AuNPs, which led to the changes in the dielectric constant of the interface. The effects were reflected in pronounced shifts of the plasmon angle, $\theta_p$, in the SPR spectra. In case of the GOx/AuNP system bridged to Au support by the long dithiol monolayer, a shift of $\theta_p$ (39′) was

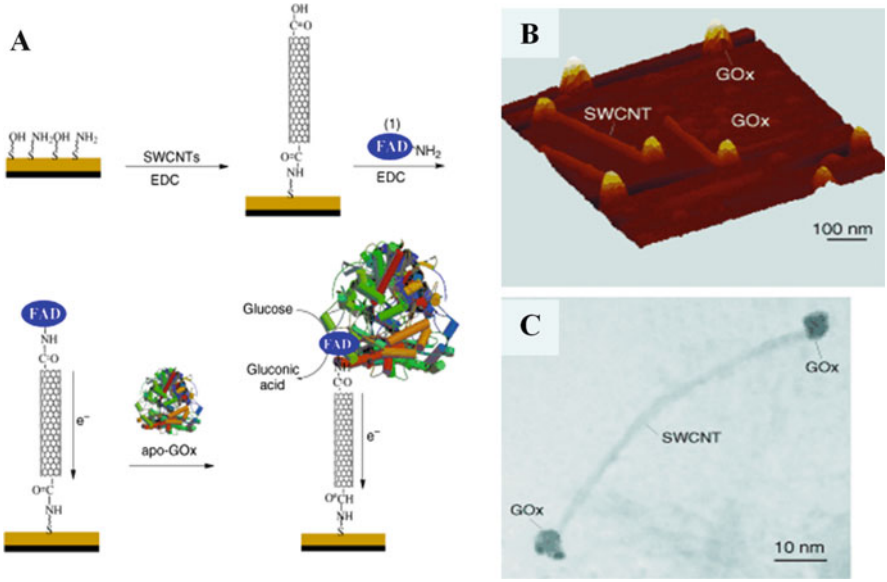


**Fig. 4** (**A**) Assembly of the SWCNT electrically contacted GOx electrode. (**B**) AFM image of SWCNTs reconstituted at their ends with GOx units. (**C**) HRTEM image of a SWCNT modified at its ends with GOx units. Adapted with permission from [24]. Copyright (2004) WILEY-VCH Verlag GmbH & Co.

observed before and after addition of glucose. Whereas, in analogous system, which was bridged with the short dithiol monolayer, a smaller change $\theta_p$ (27′) was observed before and after addition of glucose. Thus, the changes in the plasmon angles were more pronounced in the long dithiol system, as compared to the short dithiol system. Charging of the AuNPs associated with the interface also resulted in changes of the double-layer capacitance. The potentials of the aligned GOx/AuNP-modified electrodes, prior to the addition of glucose, were close to the zero-charge potential values and thus provided the minimum values of $C_{dl}$. Upon addition of 100 mM of glucose, the capacitance increased from ca. 2.1 to 3.6 μF $cm^{-2}$ ($\Delta C_{dl}$ ~80%) for longer dithiol monolayer. In contrast, the change was lesser for shorter dithiols from ca. 19 to 24.7 μF $cm^{-2}$ ($\Delta C_{dl}$ ~22%). These results were consistent with the larger shift of $\theta_p$ observed in the SPR measurements in the presence of the long dithiol linker as compared to the changes observed with shorter dithiol. The long dithiol linker yielded a densely packed monolayer which provided an effective tunnelling barrier for the transport of electrons from the AuNPs to the bulk Au electrode. This resulted in the effective charging of the AuNPs reflected by the significant changes of the interfacial capacitance. In contrast, the short dithiol linker allowed the leakage of electrons from the AuNPs to the bulk Au electrode, resulting in diminished charging of the AuNPs. As a result only moderate changes in the capacitance values of the interface were observed. A control for GOx/AuNP hybrid where GOx was unspecifically linked to AuNPs did not show significant changes in

plasmon angle or capacitance after addition of glucose. The studies showed that the electrocatalytic efficiency of GOx reconstituted over electrically connected FAD was considerably enhanced when compared to a non-aligned assembly.

*Protein engineering* has long been used to alter the native protein structures to acquire desired functions which could be exploited for their electrochemical applications. These desired functions could be increased sensitivity of engineered redox proteins towards their substrate, ease of their immobilisation over the electrode surface with added stability and/or enhanced electron transfer efficiency [51]. Different approaches are used for redox protein engineering [11]. Rational design is one of the commonly used approach where the existing extensive knowledge of protein structure–function and computational modelling are combined together either to chemically synthesise de novo proteins with desired functionalities or to accurately modify native protein structure (either by controlled digestion of amino acids or by point mutations to alter amino acid sequence) to tune the redox (or other desired) properties of proteins. In contrast to this approach, directed evolution does not require the prior knowledge of protein structural data and the relationship between sequence, structure and mechanism for generation of mutants. Instead, a library of variants is created by iterative rounds of mutagenesis of the target gene that are then selected and screened till the desired functions are acquired. Molecular "lego" is another approach to engineer redox proteins where the proteins with desired properties are fused together [52]. The molecular lego mimics the natural molecular evolution which is proceeded by modular assembly of genes/DNA segments. The key domains or building blocks are selected to assemble artificial redox chains with the desired properties, ultimately capable of communicating with the electrodes. The link between protein domains can be achieved by a peptide linker or by a disulphide bridge between the two domains. To ensure efficient electron transfer between the two domains and ultimately with the electrode, the position and length of the linkers are chosen in such a way that the association complexes are favoured, allowing optimal electron transfer.

One of the most popular examples of rational design approach to engineer a redox protein for its electrochemical application was trimming of cyt c by controlled enzymatic digestion to yield microperoxidase-11 (MP-11). The heme redox centre in cyt c was exposed in MP-11 for better electron coupling with the electrode. The approach of rational design has also been used to selectively modify protein surface structure for ease of immobilisation over electrode surface (e.g. introduction of surface-exposed histidine or cysteine for cross-linking or self-assembly over electrode, respectively) [53]. In another example, Willner and co-workers [17] reconstituted a de novo synthesised four-helix bundle with $Fe^{III}$ protoporphyrin IX moiety wired over the functionalised Au electrode and explored its electrochemical properties. The reconstituted helical protein showed efficient electron transfer with the electrode and acted as an artificial heme cofactor that substituted cyt c in activating cyt c-dependent enzymes like nitrate reductase (from *E. coli*). In one of the recent studies, Marshall et al. [54] predictably and rationally tuned the $E^{\circ\prime}$ of cupredoxin azurin (Az) to the full range $706 \pm 3$ mV at pH 4 for N47S/F114N/M121L Az variant to $-2 \pm 13$ mV at pH 9 for F114P/M121Q Az

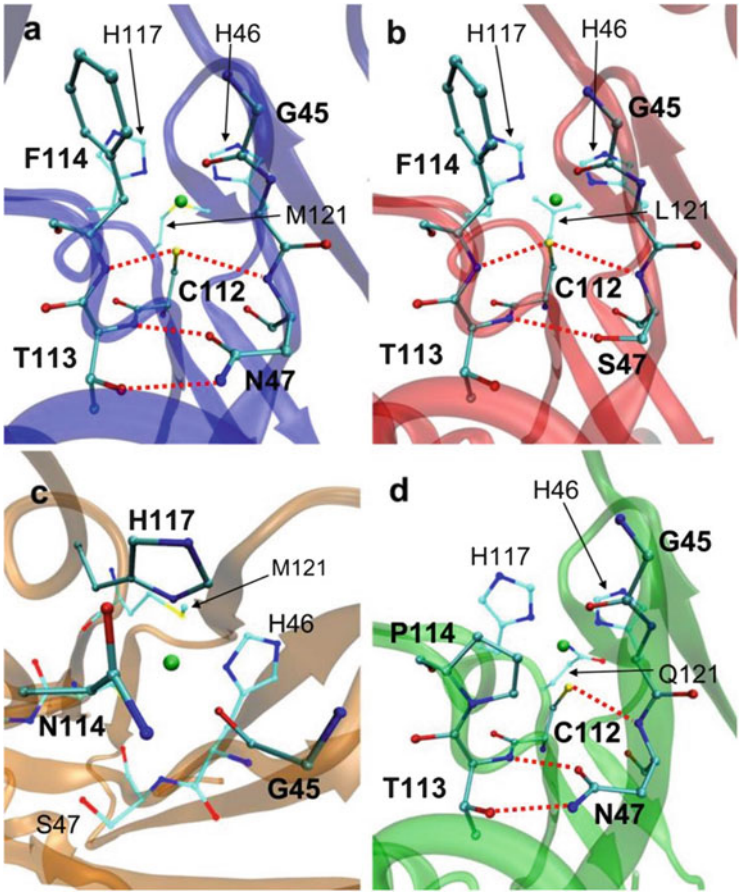


**Fig. 5** X-ray structures of Az and selected variants. (**a**) Native Az (PDB 4AZU). (**b**) N47S/M121L Az: N47S affects the rigidity of the copper binding site and, probably, the direct hydrogen bonds between the protein backbone and Cys 112. (**c**) N47S/F114N Az: introducing a hydrogen bond donor at position 114 perturbs hydrogen bonding near the copper binding site, possibly disrupting donor–acceptor interactions to His 117 or ionic interactions between the copper and the carbonyl oxygen of Gly 45. (**d**) F114P/M121Q Az: F114P deletes a direct hydrogen bond to Cys 112 resulting in a lower redox potential. In all panels copper is shown in *green*, carbon in *cyan*, nitrogen in *blue*, oxygen in *red* and sulphur in *yellow*. Hydrogen-bonding interactions are shown by *dashed red lines*. Adapted with permission from [54]. Copyright (2009) Nature Publishing Group

variant surpassing the highest and lowest reduction potentials reported for any mononuclear cupredoxin. This unprecedented level of control over an electron transfer protein was achieved by mapping out major interactions in protein structure followed by their selective modification, an approach that could be extended to all other redox proteins (Fig. 5). Such proteins with wide redox potential and pH ranges are useful as biosensor or biofuel cell catalysts. Other attempts at protein

engineering involved directed evolution to enhance the catalytic efficiency and stability and to modify substrate specificity in CYP variants from different sources [55, 56]. The manyfold increased sensitivity towards various environmental pollutants and drugs makes these variants a potential target for biosensor applications.

### *3.4 To Aid in Miniaturisation of Bioelectrochemical System*

The combination of biological molecules and novel nanomaterial components is of great importance in the process of developing new nanoscale devices for future biological, medical and electronic applications. Recent studies show a tremendous increase in the use of nanomaterials for bioelectrochemical applications. The reasons are high surface to volume ratio provided by these nanomaterials over the transducer surface (aiding in the increased protein loading that results in higher sensitivity and lower detection limit), their fast electron transfer efficiency, their specific electronic and optical properties and their ease of availability. A lot of research has been published lately exploring the utility of nanomaterials for electrochemical studies of redox proteins and their applications in biosensing and biofuel cells.

*Nanotubes and nanowires* are extensively used immobilisation matrices for electrochemical studies of redox proteins. The group includes mostly carbon, silicon, conducting polymer, metallic (Au, Pt, Ni) and semimetallic ($TiO_2$ [57], ZnO [58]) nanotubes or nanowires. They are also termed as one-dimensional (1-D) nanostructures because of a high ratio of their length (μm) to their diameter (nm). Synthesis, characterisation and alignment of these 1-D structures for their biosensor applications have been extensively reviewed [59, 60]. Since most of these nanowires are commercially available, a detailed description of synthesis and characterisation are either consciously avoided or only briefly discussed in the context of examples in this section. However, there are many research groups which focus on synthesising these nanowires for their tailor-made applications.

Among 1-D structures, carbon nanotubes (CNTs) are the most popular ones. The physical and catalytic properties make CNTs ideal for use in sensors. Most notably, CNTs display high electrical conductivity, chemical stability and mechanical strength. The two main types of CNTs are single-walled CNTs and multi-walled CNTs. SWCNTs are $sp^2$-hybridised carbon in a hexagonal honeycomb structure that is rolled into a hollow tube morphology. MWCNTs are multiple concentric tubes encircling one another. SWCNTs can be classified as either semiconducting or metallic allotropes, depending on the chirality. CNTs are primarily synthesised by three main techniques: arc discharge, laser ablation/vaporisation and carbon vapour deposition (CVD). Most commercially available CNTs are formed by CVD. After synthesis, CNTs may be treated to functionalise their surfaces. The most common treatment with strong acids removes the end caps and may also shorten the length of the CNTs. Acid treatment also adds oxide groups, primarily carboxylic acids, to the tube ends and defect sites. Further chemical reactions can be performed

at these oxide groups to functionalise with groups such as amides, thiols or others. Altering the nanotube surface strongly affects solubility properties, which can affect the ease of fabrication of CNT-based sensors. A recent review by Jacobs et al. [61] compiled detailed accounts of CNT-based electrochemical sensors for biomolecule detection. A large number of studies have focused on immobilisation of GOx in nanocomposite films of SWCNTs/MWCNTs dispersed in chitosan/NF/PPy for fast and sensitive electrochemical detection of glucose. Besides GOx, other enzymes such as lactate oxidase, lactate dehydrogenase, galactose oxidase, cholesterol oxidase, alcohol dehydrogenase, etc. have also been immobilised in CNT nanocomposite for the detection of biologically important molecules. CNTs are also frequently used as immobilisation matrix for heme-containing proteins. Yang et al. [25] developed a method to directly bind Hb to diazonium-modified aligned CNTs (ACNTs) via carbodiimide chemistry. The aligned nanotube forest resulted in greater surface coverage ($\Gamma = 2.7 \times 10^{-9}$ mol cm$^{-2}$) for Hb resulting in higher catalytic current when compared to immobilisation in random tangled webs of CNTs. SEM and FTIR spectroscopy were used to characterise the ACNTs and Hb-ACNTs (Fig. 6A and B). The ACNTs showed partially opened tip and uniform, straight and smooth sidewalls with average outer diameter of ca. 50 nm (Fig. 6A, a, b, c). Figure 6A, d, e, f shows the ACNT arrays after diazonium reaction and covalent immobilisation of Hb molecules. Sidewall roughness and closed tips showed that the Hb was immobilised both on sidewalls and the tips of ACNTs (Fig. 6A, e, f). The FTIR spectrum for Hb-ACNT showed (Fig. 6B, d) two typical peaks at 1,656 and 1,546 cm$^{-1}$, which contributed to the C=O stretching vibration of amide I band and the combination of N–H bending and C–N stretching vibration of amide II band, respectively. The bands showed only a slight redshift after immobilisation on ACNTs when compared to the natural Hb peaks at 1,652 and 1,540 cm$^{-1}$ (Fig. 6B, c), indicating that the interaction of Hb with diazonium-ACNTs did not destroy the native secondary structure of Hb. The Hb film on the diazonium-ACNTs electrode showed well-defined redox peaks with $E^{\circ\prime}$ at −312 mV (vs. Ag/AgCl) and good electrocatalytic activity for $H_2O_2$ reduction. The Hb-ACNTs electrode exhibited high sensitivity, long-term stability and wide concentration range from 40 μM to 3 mM for the amperometric detection of $H_2O_2$. The fact that vertically aligned nanotube forests had better kinetics for direct electron detection was further established by Esplandiu et al. [62]. They immobilised myoglobin over vertical ACNTs to detect either $H_2O_2$ or $O_2$ separately. CNT forests showed superior kinetics when compared to nanocomposite epoxy-incorporated SWCNTs/myoglobin sensors. A higher limit of detection of ~50 nM was recorded for $H_2O_2$, superior to other previously reported random and aligned nanotube methods.

Among metallic nanowires, gold nanowires (AuNWs) are fast gaining ground in the biosensing applications due to their high chemical and thermal stability, biocompatibility and excellent electrical conductivity [63, 64]. Their ease of self-assembly over thiol-modified transducer surfaces provides a stable matrix for biomolecule assembly. The self-assembled AuNWs can then be functionalised to acquire free amino or carboxyl groups for protein cross-linking. While a number of

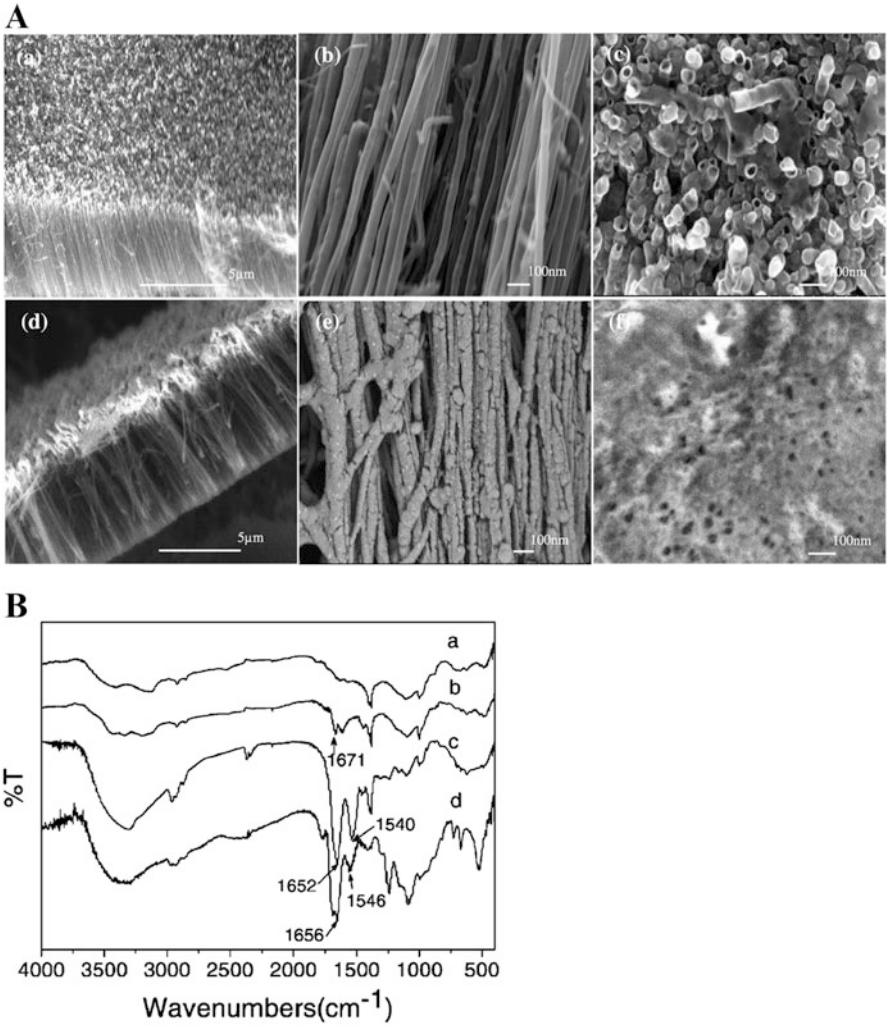


**Fig. 6** (**A**) SEM images of ACNTs (*a*, *b*, *c*) and Hb-ACNTs (*d*, *e*, *f*). (**B**) IR spectra of (*a*) ACNTs, (*b*) diazonium-ACNTs, (*c*) Hb and (*d*) Hb-ACNTs film. Adapted with permission from [25]. Copyright (2009) WILEY-VCH Verlag GmbH & Co.

techniques for AuNWs fabrication have been reported, electron beam lithography [64] and electrodeposition in alumina template [65] are frequently used. Sometimes they are fused together with platinum or nickel to change the functionality [65].

Recent trends suggest increasing use of conducting polymer nanowires such as PPy, PANI and poly(ethylene dioxythiophene) (PEDOT) and their functionalised derivatives as immobilisation matrix for redox proteins. Ease of synthesis of conducting polymer nanowires and their in-built functional groups give them an edge over other inorganic nanowires where addition of functional groups for redox

protein immobilisation is always an additional step. Among the methods used for fabrication of conducting polymer nanowires are template-assisted synthesis, photolithography and e-beam lithography, dip-pen nanolithography, hydrodynamic focusing and direct electrochemical synthesis [66]. Wang et al. [67] reported an amperometric glucose biosensor based on the direct electron transfer of GOx by electrochemically entrapping GOx onto the inner wall of highly ordered PANI nanotubes (PANI-NTs). PANI-NTs were synthesised using anodic aluminium oxide (AAO) membrane as a template. Figure 7A shows SEM images of highly ordered PANI-NTs with the outer diameter of 250–300 nm and the inner diameter of ~150 nm. Inset of the Fig. 7A is the top view showing the open ends of these nanotubes. The PANI-NTs thus provided an ideal size of channel to entrap GOx. The immobilised GOx is shown as small and uniformly distributed island-like nanostructures with the size of ~50 nm adhered on the inner wall of PANI-NTs (Fig. 7B). Figure 7B also shows that PANI-NTs retain the nanotube structure after GOx immobilisation, an important characteristic to enable free and fast diffusion of substrates and products inside the nanotubes. GOx immobilised in PANI-NTs showed a pair of well-defined and nearly symmetrical redox peaks in CV with the anodic and cathodic peak potentials at −390 and −420 mV, respectively, with $\Delta E_p = 30$ mV. The apparent $k_s$ was estimated to be $5.8 \pm 1.6\ s^{-1}$. In addition, the GOx/PANI-NTs/Pt electrode showed higher sensitivity ($97.18 \pm 4.62\ \mu A\ mM^{-1}\ cm^{-2}$), lower detection limit ($0.3 \pm 0.1\ \mu M$) and faster response time (~3 s) with considerable stability when compared to other reported glucose biosensors.

*Nanoparticles and microparticles* constitute a diverse class of materials frequently used for immobilisation of redox proteins. The commonly used are metallic nanoparticles (Au, Ag, Pt), conducting polymer nanoparticles, silica microparticles, etc. The obvious advantages are high surface to volume ratio, thus allowing higher protein loading and aiding miniaturisation besides their efficient conductivity and stability as a matrix for protein immobilisation. Metallic nanoparticles, especially AuNPs are increasingly being used for protein electrochemical studies. Similar to

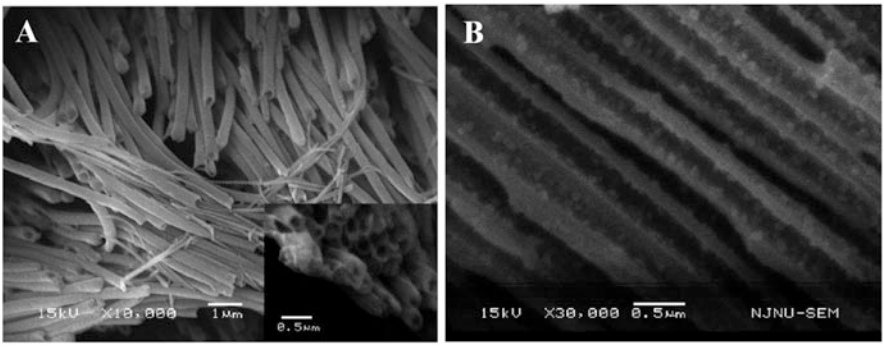


**Fig. 7** (**A**) SEM images of PANI-NTs obtained by etching away the AAO membrane. (**B**) The cross-sectional image of the PANI-NTs after loading GOx on the inner wall of the nanotubes. Adapted with permission from [67]. Copyright (2009) American Chemical Society

AuNWs, the ability of AuNPs to self-assemble over a thiol-modified surface provides a stable matrix for protein immobilisation. Furthermore, because of their efficient electron conductivity, they permit direct electron transfer between redox proteins and bulk electrode, thus allowing electrochemical sensing to be performed without the need of electron transfer mediators. AuNPs have also demonstrated to constitute useful interfaces for the electrocatalysis of redox processes of molecules such as $H_2O_2$, $O_2$ or NADH involved in many significant biochemical reactions. One recent review by Pingarron et al. [68] provides a detailed account on the use of AuNPs for immobilisation and electrochemical studies of various proteins including GOx, horseradish peroxidase, Hb, myoglobin, etc. In an interesting approach, Melin et al. [69] compared the effect of size of AuNPs on electrochemistry of cbo3. AuNPs of sizes 15, 38 and 56 nm were drop casted on a series of gold electrode surfaces, and their surface areas were compared electrochemically by integration of the Au–O reduction peak at 1.1 V. Although the overall surface area increased with AuNP layer, it decreased with increasing size of AuNPs from 15 to 5.5 and 2.5 $cm^2$, respectively. The electrocatalytic peak potential of cbo3 also shifted towards more negative values with increasing nanoparticle size, meaning smaller AuNPs apparently allowed faster electron exchange rates with this enzyme.

Recently, nanoparticles with magnetic properties have also been used for protein immobilisation and their electrochemical studies [70, 71]. They usually contain a metal or metal oxide core of iron or cobalt. The magnetic core is often stabilised by an outer inorganic or organic shell, such as silica [71], carbon [70], etc. where the redox proteins are directly adsorbed. It is possible to further modify these magnetic nanoparticles by anchoring different functional groups to their outer shell to serve specific functions. For example, addition of charged polymers such as PEI increases the solubility of these magnetic nanoparticles in aqueous solutions [72]. Besides, they also provide additional functional groups that can be used for protein cross-linking.

*Graphene* is also among one of the important carbon materials used for the electrochemical studies of redox proteins. The unique properties of graphene (fast electron transportation, high thermal conductivity, excellent mechanical flexibility and good biocompatibility) provide it with potential applicability in electrochemical biosensors as summarised by Kuila et al. [73] in one of their recent reports.

## 4 Applications

The efficient confinement of the redox proteins over the transducer surfaces opens the way for their various electrochemical applications with high precision and reproducibility.

## 4.1 Study of Mechanism

Applications of electrochemical methods in investigation of mechanism of redox protein catalysis have greatly increased in the past few years, as confidence has grown in their ability to provide alternative new insight into complex electron transfer processes [4, 74]. Electrochemical studies of redox proteins have contributed a lot towards understanding enzyme kinetics, substrate binding and structure–function relationships in proteins. Some of the recent examples are elaborated in this section to understand the contributions. As discussed before, CYP is an enzyme whose electrochemical investigation has a huge application potential. However, catalytic cycle of CYP is quite complex which makes its electrochemical investigation quite intriguing [75]. Hagen et al. [27] investigated the CYP 2B4 electrochemistry in DDAB films. The variation of $E^{\circ\prime}$ with a range of temperature from 18°C to 40°C was used to measure the entropy and enthalpy changes that accompany heme reduction in CYP 2B4 to understand the nuclear reorganisation of the enzyme. Reduction of six-coordinate water-ligated $Fe^{III}$ yields five-coordinate $Fe^{II}$ and expulsion of the axial water ligand [74]. The corresponding changes in entropy ($\Delta S^{\circ}$) and enthalpy ($\Delta H^{\circ}$) values were $-151$ J mol$^{-1}$ K$^{-1}$ and $-46$ kJ mol$^{-1}$, respectively. To further probe the effect of dehydration, on entropy and enthalpy changes, similar electrochemical experiments with CYP 2B4-DDAB films in the presence of imidazole in solution were performed. Imidazole replaces water as the heme axial ligand and remains bound to the heme in both $Fe^{III}$ and $Fe^{II}$ oxidation states, unlike water which dissociates upon reduction. The values for $\Delta S^{\circ}$ and $\Delta H^{\circ}$ were calculated to be $-59$ J mol$^{-1}$ K$^{-1}$ and $-18$ kJ mol$^{-1}$, respectively, significantly smaller than the water-ligated CYP 2B4. This dramatic difference was explained with the likely structural rearrangements that accompanied these two redox reactions. Reduction of a six-coordinate axially aquated heme triggered water dissociation, whereas reduction of an imidazole-bound heme produced no change in coordination, thus causing minimal nuclear reorganisation resulting in small entropy and enthalpy changes.

Lately, electrochemical studies of redox enzymes are frequently being used to gain significant insight into the enzyme kinetics. They add a new dimension called potential (V) to the familiar substrate concentration ([s]) and time (t) dimensions in the usual enzyme kinetics. The enzyme kinetic studies by electrochemical methods have also benefited from the ability of these methods to utilise extremely small quantities of enzyme sample on an electrode [74]. Fourmond et al. [76] used PFV to examine the kinetics of nitrate reduction by periplasmic nitrate reductase (NapAB) from *Rhodobacter sphaeroides*. The enzyme reversibly interconverts between active and inactive states. In their study, protein film voltammetry proved invaluable for detecting these states and determining the conditions under which they are produced. NapAB was adsorbed on pyrolytic graphite edge (PGE) electrode, and a fast and direct electrochemistry was observed with the activity detected as a negative current with peak potential at $-100$ mV (Fig. 8a, A). However, the catalytic voltammograms recorded with higher nitrate concentrations exhibited a

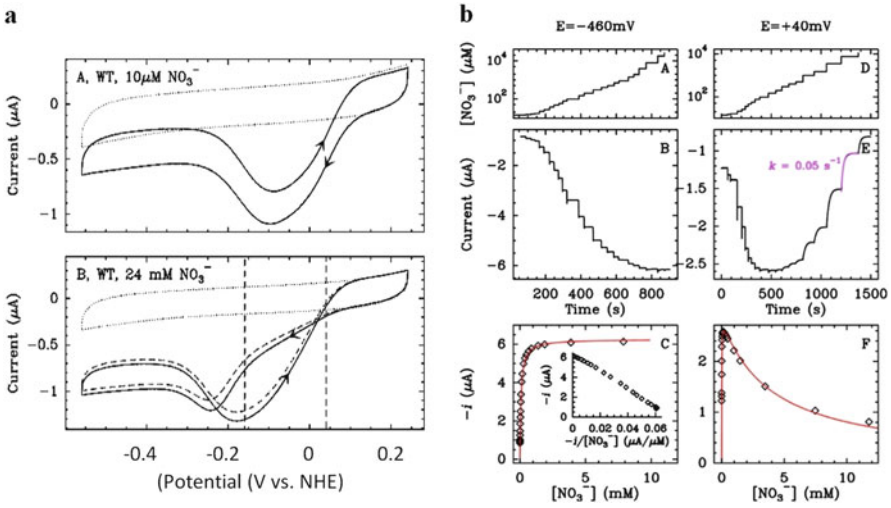


**Fig. 8** (**a**) CVs of NapAB adsorbed on a rotating disc PGE electrode, at pH 6, 25°C, a scan rate of 20 $mVs^{-1}$ and an electrode rotation rate of 5 krpm. *Panel A* shows the usual steady-state catalytic response obtained in the presence of 10 μM nitrate (*plain line*); the *dotted line* is a blank recorded with no adsorbed enzyme. The *arrows* indicate the direction of the sweep. *Panel B*: a large hysteresis is visible at high nitrate concentration (24 mM). The *dashed line* is the scan following immediately the *solid line*; the only difference is a decrease in the amplitude of the signal due to film loss. (**b**) Dependence of the rate of nitrate reduction on nitrate concentration. The left- and right-hand sides correspond to a redox poise at −460 and +40 mV vs. SHE, respectively. Conditions: pH 6; 25°C; 5 krpm. *Panels A* and *D* show the evolution of nitrate concentration against time, when the concentration is stepwise increased by adding aliquots of a stock solution of potassium nitrate (note the logarithmic Y scale). *Panels B* and *E* show the resulting change in catalytic current. *Panels C* and *F* show the catalytic current reached at the end of each step as a function of nitrate concentration. The fit of the data in *panel C* to the Michaelis–Menten equation gives $K_m = 85$ μM. The *inset* shows an Eadie–Hofstee plot. The *red line* in *panel F* is the best fit to an equation accounting for substrate inhibition, with $K_m = 10$ μM and $K_i = 4$ mM. Adapted with permission from [76]. Copyright (2010) American Chemical Society

pronounced hysteresis above −200 mV (Fig. 8a, B), and the current measured during the forward scan (towards negative potentials) was smaller than that during the return scan. Chronoamperometric experiments were carried out to understand this phenomenon by stepwise varying the substrate concentration at two different potentials, and the resulting change in activity was monitored as a change in current (Fig. 8b). At very low electrode potential ($E = -460$ mV) (Fig. 8b, A, B, C), the catalytic activity increased with increasing nitrate concentration and followed Michaelis–Menten kinetics. However, under less reductive condition ($E =$ +40 mV) (Fig. 8b, D, E, F), high concentrations of nitrate inhibited the enzyme. The experiments showed that reduction activated NapAB irreversibly, whereas at moderately reducing potentials, high nitrate concentrations reversibly inhibited the enzyme.

Chronoamperometry allows for the study of enzyme kinetics with great temporal resolution which is useful for the study of reactions involving substrate (especially gaseous substrates) binding and depletion with time. Hydrogenases, which catalyse $H_2$ to $H^+$ conversion as part of the bioenergetic metabolism of many microorganisms, are among the metalloenzymes for which the existence of a gas-substrate tunnel is already reported (by crystallography and molecular dynamics methods). However, the correlation between protein structure and gas diffusion kinetics remains unexplored. Leroux et al. [77] used chronoamperometry to resolve the kinetics of binding and release of the competitive inhibitor CO in structurally characterised mutants of a NiFe hydrogenase (Fig. 9a and b). As shown in Fig. 9a, the mutations L122M-V74M (MM) and L122F-V74I (FI) significantly narrow the tunnel near the entrance of the catalytic centre. Since CO substitutes for $H_2$ at the active site of NiFe hydrogenase in a competitive manner, PFV was used to monitor $H_2$ oxidation to measure the rates of binding and release of the competitive inhibitor CO with high temporal resolution. In the wild-type (WT) enzyme at room temperature, binding of CO was fast (Fig. 9b, A); it is just below the diffusion limit of $10^8\ s^{-1}\ M^{-1}$ [$\sim 10^5\ s^{-1}$ atm $(CO)^{-1}$; the solubility of CO is 0.96 mM $atm^{-1}$]. The two double mutations induced spectacular delays in both binding and release of CO (Fig. 9b, B and C). The rate constants for both forward and backward CO transport decreased by more than two orders of magnitude in MM mutant, whereas the double FI mutant had an intermediate phenotype. Since the mutations affect the rates of CO binding and release in approximately the same

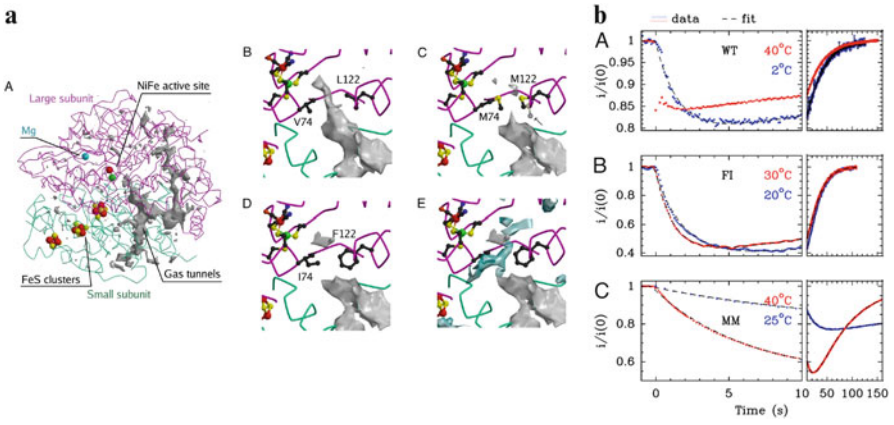


**Fig. 9** (**a**) Structural models of the three enzymes. *A* is an overview of the tunnel network; *B* is a close-up of the tunnel near the active site in the WT. *C*, *D* and *E* are close-ups of the MM and FI mutants, as indicated. In *C*, an arrow points to the second conformation of M122. A conserved hydrophilic cavity is shown in *blue* in *E*. (**b**) Comparison of the kinetics of CO inhibition of $H_2$ oxidation in PFV experiments. The current ($i$) has been normalised by its value $i_0$, measured before CO was added. *Left* shows the short-term change in current, whereas the end of the relaxation is shown on *Right*. The dimensionless volumic fractions of solutions saturated under 1 atm of CO at 25°C and injected at time 0. Electrode rotation rate 2 krpm, pH 7. Adapted with permission from [77]. Copyright (2008) PNAS

manner, they had a smaller effect on the binding affinity, which is the ratio of the two. This was expected for a mutation that affects the channel for CO access, but not the free energy of binding at the active site. Thus electrochemical studies established the effect of mutations affecting the molecular structure of substrate tunnels in hydrogenase enzyme. In fact, electrochemical studies of redox proteins are now fast becoming an inevitable tool to establish or support structure–function findings [78–80].

## *4.2 Biosensors*

Biosensors are the most practical and important applications where developments in electrochemical studies of redox proteins have played a major role. In the last decade, a substantial part of these studies were directed towards biosensing applications. However, most of these biosensing devices were of lab scale that are yet to be optimised for real-world applications. Sensors in general are devices that register a physical, chemical or biological change and convert them into a measurable signal. They usually contain a recognition element which detects the analyte of interest, a transducer that produces the signal and a processor that collects, amplifies and displays the signal. Electrochemical biosensors are a class of sensors that combine the sensitivity and selectivity of biological components (especially enzymes) with low detection capabilities of electrochemical transducers ($\sim 10^{-12}$ A current). The biosensor performance is usually evaluated on the basis of its selectivity, sensitivity, limit of detection (LOD), reproducibility, response time, operational and storage stability, ease of use and portability. With the onset of electrochemical biosensors in 1960s and subsequent development of glucose biosensors for blood glucose analysis, a volume of literature has been published in last 50 years. Some of the recent reviews have covered the details about the enzymatic biosensors including their working principal, design, selection of biocatalyst and immobilisation strategies for biocatalysts over electrodes followed by their usage and performance for clinical, environmental and industrial applications [5, 81–86].

Electrochemical biosensors have found their potential applications in clinical diagnostics. The substrate specificity (selectivity) and sensitivity of enzymatic biosensors avoid a great deal of sample preparation when analysing complex biological fluids such as blood or urine. In Sect. 3, we have already seen that many of the immobilisation strategies were directed towards the development of glucose biosensor for blood glucose analysis. However, the studies on glucose biosensors are consciously eluded here in this section as this book contains an independent chapter focused on glucose biosensors. After glucose, cholesterol is one among the important analytes in blood that requires frequent monitoring. It is an important biomarker in the diagnosis of many diseases, such as hypertension, coronary heart disease, arteriosclerosis, lipid metabolism dysfunction, etc. This has led to an increased interest in the development of various kinds of cholesterol biosensors [87]. Saxena et al. [88] developed a cholesterol oxidase (ChOx)

bioelectrode and established its potential as biosensor for total cholesterol determination in human serum samples. ChOx was immobilised on AuNP-modified gold electrode. The nanoparticle film on the electrode surface provided an environment for the enhanced electrocatalytic activity of ChOx and thus resulted in enhanced analytical response. The resulting bioelectrode exhibited a linear response to cholesterol in the range of 0.04–0.22 mM with a detection limit of 34.6 μM and a high sensitivity of 9.02 μA $mM^{-1}$ at a working potential of 0.46 V. A high operational (6 h, 30 measurements) and storage stability (~95% residual activity after 1 month of storage) was reported for this ChOx-based biosensor. A recent report by Saxena and Das [89] summarised the progress in designing and fabrication of cholesterol biosensors using nanomaterials and their importance in clinical studies.

In addition to clinical diagnostic applications [84, 85], enzymatic biosensors have also made a lot of progress in environmental applications [81, 86] such as for detection of various pollutants, pesticides, heavy metal contaminations of groundwater, etc. to name a few. The monitoring of arsenite, the major contributor of groundwater arsenic contamination, is among one of the major environmental concerns that requires immediate attention. Arsenite oxidase (ArO), a molybdenum-containing enzyme, is responsible for arsenite utilisation in a large number of microorganisms, e.g. *Rhizobium* sp. str. NT-26, *Alcaligenes faecalis*, etc. The arsenite utilisation pathways in these organisms make use of arsenite as the electron donor and molecular oxygen as the terminal electron acceptor. Despite having a huge potential for biosensor applications for one of the most dreaded pollutants of water, ArO was largely ignored in terms of its electrochemical studies. The reason could again be attributed to the enzyme being dimeric and bulky (heterologous subunits: molybdenum-containing Aro A, MW ~90 kDa, and Rieske-type Fe–S-containing Aro B, MW ~15 kDa) [90]. However, a biosensor for arsenite was developed using ArO (from *Rhizobium* sp. str. NT-26) that oxidises arsenite to arsenate. ArO was galvanostatically deposited onto the active surface of a MWCNT-modified GCE. The resulting biosensor showed a linearity up to 500 ppb and a detection limit of 1 ppb for arsenite at 0.3 V electrode potential. A low response time (~10 s) and excellent reproducibility were reported for the ArO biosensor. The biosensor was used for repeated analysis of spiked arsenite in tap water, river water and commercial mineral water. River water from the St. Lawrence River was analysed using the ArO biosensor (Fig. 10). The results implied that arsenite was not present in the river water, since the current signal (~17 nA) for curve b was very similar in the presence or absence of ArO (Fig. 10A and B). The results were later confirmed by other established methods for arsenite determination.

Enzymatic biosensors also have potential applications in the food industry to detect the analytes which should be in permissible levels, e.g. peroxides, sulphites, etc. Sulphite is used as an additive in food and beverages to prevent oxidation and bacterial growth and to control enzymatic reactions during production and storage. The level of sulphite is the subject of legislation because it can cause asthmatic attacks and allergic reactions to hypersensitive people. Wollenberger and

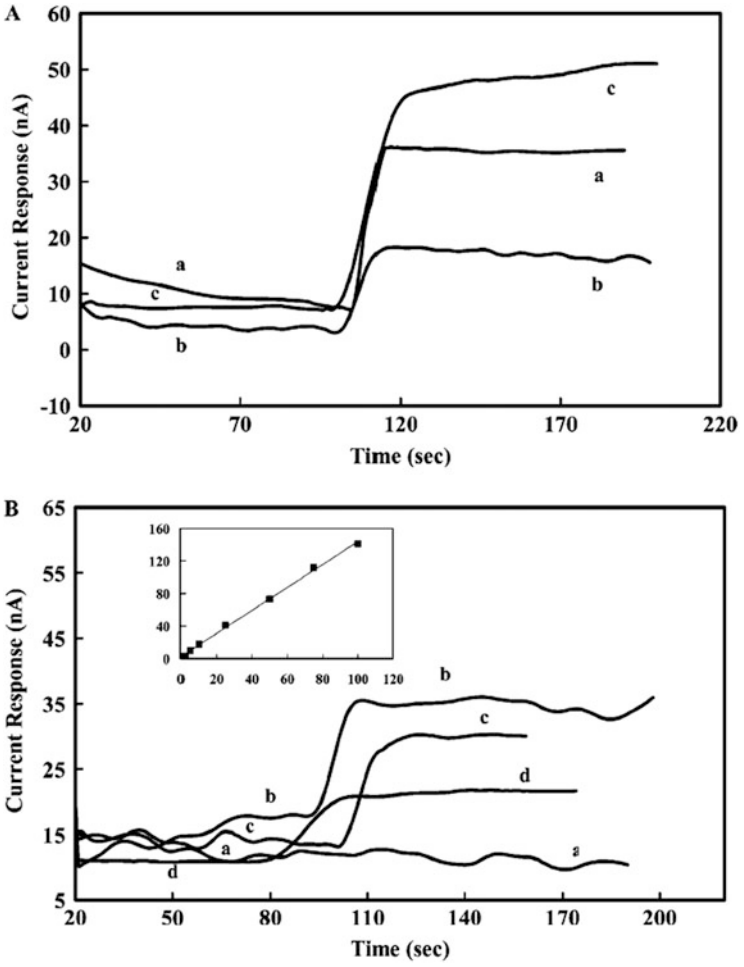


**Fig. 10** (**A**) St. Lawrence River water analysis with MWCNTs/ArO/GCE (*a*) 20 ppb arsenite, (*b*) St. Lawrence River water alone and (*c*) St. Lawrence River water spiked with arsenite to give 20 ppb after mixing. (**B**) St. Lawrence River water analysis with MWCNTs/GCE (*a*) 20 ppb arsenite, (*b*) St. Lawrence River water alone, (*c*) river water spiked with arsenite to give 20 ppb after mixing and (*d*) 10 ppm humic acid. The *inset* shows a calibration curve for arsenite in the presence of the St. Lawrence River water. Adapted with permission from [90]. Copyright (2007) American Chemical Society

co-workers [91] developed sulphite biosensor using human sulphite oxidase (hSO) enzyme, a metalloprotein containing the molybdenum cofactor and a cytochrome b5-type heme. In a layer-by-layer assembly method, the hSO was co-immobilised with cyt c in polyaniline sulphonic acid. A 17-bilayer electrode showed a linear range between 1 and 60 μM sulphite with a sensitivity of 2.19 mA $M^{-1}$ sulphite and a response time of 2 min. The multilayer electrode was used for determination of sulphite in unspiked and spiked samples of red and white wine.

The recent developments in electrochemical studies of redox enzymes have opened a whole new horizon for biosensor development for a variety of analytical applications. However, a lot of research is still required to find potential biocatalysts for a number of analytes that need constant monitoring and to make electrochemical biosensors commercially successful bioanalytical device.

## *4.3 Biofuel Cells*

In addition to biosensors, biofuel cells are another important devices benefitting from the recent progress in electrochemical studies of redox proteins. With the increasing energy demand and depleting non-renewable energy resources, it is important to shift our focus to utilise renewable resources. Biofuel cells provide one such alternative, where microbes or isolated enzymes are used to utilise fuels such as glucose, fructose, lactose, ethanol, methanol, $H_2$, etc. for energy generation. Microbial fuel cells provide certain advantages over enzymatic fuel cells (EFCs), e.g. longer lifetime, capability of complete oxidation of fuel, etc. They are however limited by low power densities and lack of substrate specificities which necessitate the use of membrane separator in microbial fuel cells. EFCs are used to overcome the shortcomings of microbial fuel cells by providing better substrate specificity and higher power densities. EFCs also provide certain edge over inorganic catalyst-based chemical fuel cells, e.g. the overpotential of EFCs is usually close to zero, they have the ability to scavenge fuel and oxidant from ambient environment (even when they are present in trace concentrations) and they are feasible to be used in disposable and completely biodegradable devices. However, EFCs drastically lag behind the chemical fuel cells in the amount of power produced and their shelf life. The time and cost of isolation and purification of enzymes, their poor stability and restricted pH and temperature optima for functioning and difficulty in achieving good electronic coupling with the electrode are other serious limitations of EFCs. The focussed research towards finding novel biocatalysts from natural resources or engineering the available enzymes to generate improved biocatalysts combined with the efficient immobilisation strategies of biocatalysts over electrodes has a potential to solve few of the above-mentioned problems. Some of the recent reviews [6, 7, 92–96] have detailed the developments in the field of EFCs from selection of biocatalysts and their immobilisation strategies to the design and characterisation of EFCs for their theoretical and practical applications. A wide variety of redox proteins have been employed to create unique biofuel cells that can be used in applications such as implantable power sources, energy sources for small electronic devices, self-powered sensors and bioelectrocatalytic logic gates.

Like other chemical fuel cells, EFCs have cathode-receiving oxidant and anode-receiving reductant or fuel. For most EFCs, $O_2$ is the oxidant of choice because it is freely available and has a high reduction potential, thus maximising the voltage output of the cell. The enzymes commonly used for $O_2$ reduction at cathode are blue copper oxidases such as laccase or bilirubin oxidase. Peroxidases containing iron

porphyrins are also used at cathode for reduction of $H_2O_2$. The enzymes commonly used at anode are oxidases, dehydrogenases or hydrogenases which use sugar, alcohol or $H_2$ as fuel. Some of the hydrogenases use proton as an oxidant and reduce it to produce $H_2$ at cathode. This concept is useful in identifying possible ways for renewable $H_2$ production [6]. In one of the examples, the [FeFe]-hydrogenase from *Clostridium acetobutylicum* attached to a carbon electrode was shown to be a very good catalyst for $H^+$ reduction, and this property was further demonstrated in a device in which light-dependent $H_2$ production was observed when this hydrogenase electrode was coupled to a $TiO_2$ photoanode with NADH as electron donor [97].

Habrioux et al. [98] developed a concentric glucose/$O_2$ biofuel cell. The device constituted two carbon tubular electrodes, one in the other, and combined the glucose electrooxidation at the anode and $O_2$ electroreduction at the cathode (Fig. 11A). The anodic catalyst was GOx co-immobilised with the mediator 8-hydroxyquinoline-5-sulphonic acid hydrate, and the cathodic catalyst was bilirubin oxidase co-immobilised with the mediator 2,20-azinobis(3-ethylbenzothiazoline-6-sulphonate) diammonium salt. Both enzymes and mediators were entrapped at the surface of the tubular electrodes by an electrogenerated PPy polymer. The concept of the concentric configuration was to compartmentalise the anode and cathode electrodes and to supply dissolved $O_2$ separate from the electrolyte in order to avoid secondary reactions. The dissolved $O_2$ circulated through the inside of the cathode tube and diffused from the inner to the external surface of the tube to react directly with the immobilised bilirubin oxidase. The assembled biofuel cell was studied at 37°C in phosphate buffer pH 7.4 (Fig. 11B). They further studied the influence of the thickness of the PPy polymer on the electrochemical activity of the bioelectrodes. As the enzymes were mainly adsorbed on the electrode surface of the tube rather than within the polymer film (which acted as conductive matrix to avoid enzyme linkage and the loss of mediator, Fig. 11A), the decrease in PPy thickness led to higher current density for the biocathode, whereas no real effect was observed on the catalytic electrooxidation of glucose at the anode. They also demonstrated the effect of the chemical reticulation of the enzymes by glutaraldehyde within the polymer on the performances of the bioelectrodes. In this case the bioanode showed increase in current density. The maximum power density delivered by the assembled glucose/$O_2$ biofuel cell reached 42 μW $cm^{-2}$, at a cell voltage of 0.3 V with 10 mM glucose. The results demonstrated that the concentric design of the EFC based on compartmented electrodes is a promising architecture for further development of microelectronic devices.

To overcome the limitations of partial oxidation of fuel by EFCs and to enhance their power output, Minteer and co-workers [99–101] immobilised multiple enzymes of citric acid cycle or enzymes for complete oxidation of glycerol on respective anodes. In one of the examples [101], they developed the enzymatic bioanode for complete oxidation of pyruvate, where the bioanode contained the enzymes of the Kreb's cycle (Fig. 12A). Representative power curves for the five biofuel cells containing different numbers of dehydrogenase enzymes are shown in

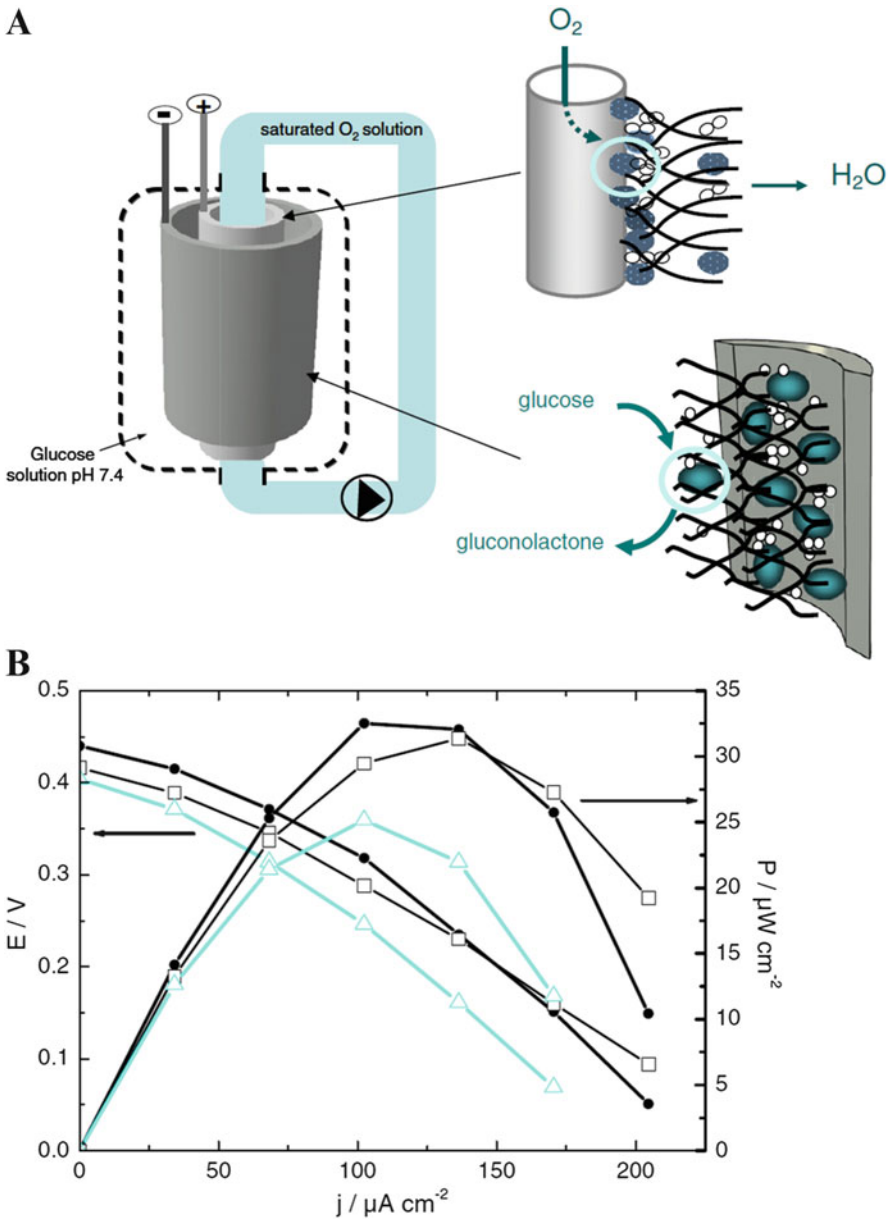


**Fig. 11** (**A**) Schematic configuration of the EFC prototype working from glucose and $O_2$ as fuel and oxidant, respectively. (**B**) Fuel cell performances obtained with the biocathode and the bioanode in a phosphate-buffered solution (pH 7.4) containing 10 mM glucose at 37°C. A saturated $O_2$ solution circulates in the interior of the inner cathode tube. (–●–) initial performances; (–□–) after 3 operating hours; (–Δ–) after 3 operating hours and 2 days of storage at 4°C. Adapted with permission from [98]. Copyright (2008) Elsevier

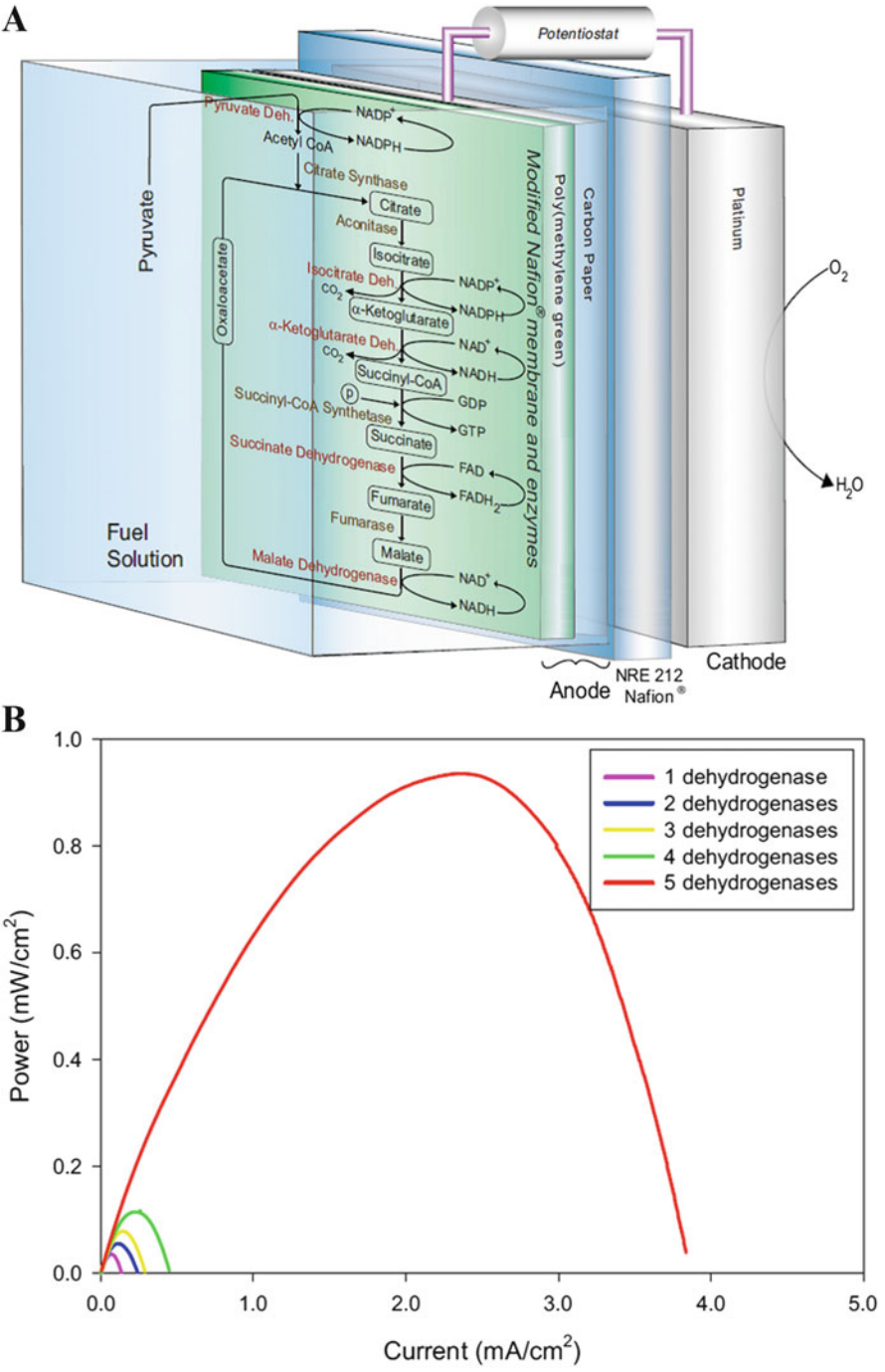


**Fig. 12** (**A**) Schematic of the chemistry occurring at the pyruvate/air biofuel cell. (**B**) Representative power curves for pyruvate/air biofuel cells in 100 mM sodium pyruvate fuel solution at room temperature. Adapted with permission from [101]. Copyright (2009) Electrochemical Society

Fig. 12B. As the number of dehydrogenase enzymes increased, the current and power density increased from $0.0298 \pm 0.0082$ mW $cm^{-2}$ to $0.931 \pm 0.091$ mW $cm^{-2}$ with 31.2-fold overall increase in power output. An overall 4.6-fold power density increase was observed using individual Kreb's cycle enzymes when compared to the intact mitochondria. These results showed that the complete oxidation of fuel could increase the power output of EFCs drastically.

## 5 Conclusions

Electrochemical studies of redox proteins have made tremendous progress in the last decade which is reflected in the literature published so far. A wide range of proteins are now being studied electrochemically, and these studies have become an integral part of protein characterisation and their structure–function studies. The constant research work dedicated towards improving the immobilisation strategies of redox proteins over electrodes for their maximum stability and electron transfer efficiency has made these studies more feasible and reproducible. Discovery and synthesis of novel materials including a variety of nanomaterials have only fuelled this progress. Recent development and use of different spectroscopic and microscopic techniques have made it possible to visualise the details at molecular level thus complementing the findings obtained by electrochemical analysis and making them more reliable. All these developments combined with the constant efforts towards improvement in stability, biocompatibility and miniaturisation of bioelectrochemical systems have established biosensors as a promising bioanalytical device for monitoring analytes of clinical, environmental and industrial importance. In addition to biosensors, the research work on enzymatic biofuel cells has also benefitted a lot from the recent progress in electrochemical studies of redox proteins. A considerable progress in stability, performance and overall power output of EFCs has been achieved. Although they still lag behind the chemical fuel cells in their power output, they are promising towards fuelling small portable and disposable devices. Thus electrochemical studies of redox proteins have become quite an interdisciplinary field of research which requires constant attention of researchers for their various theoretical and practical implications.

**Acknowledgements** I am thankful to Alexander von Humboldt Foundation for the financial support.

## References

1. Nelson DL, Cox MM (2008) Oxidative phosphorylation and photophosphorylation. In: Lehninger principles of biochemistry, 5th edn. W. H. Freeman, New York

2. Gamenara D, Seoane G, Méndez PS, Domínguez de María P (2012) Redox biocatalysis: fundamentals and applications. Wiley, Hoboken
3. Messerschmidt A, Bode W, Cygler M (eds) (2004) Handbook of metalloproteins. Wiley, Chichester
4. Léger C, Bertrand P (2008) Direct electrochemistry of redox enzymes as a tool for mechanistic studies. Chem Rev 108:2379–2438
5. Newman JD, Setford SJ (2006) Enzymatic biosensors. Mol Biotechnol 32:249–268
6. Cracknell JA, Vincent KA, Armstrong FA (2008) Enzymes as working or inspirational electrocatalysts for fuel cells and electrolysis. Chem Rev 108:2439–2461
7. Minteer SD, Liaw BY, Cooney MJ (2007) Enzyme-based biofuel cells. Curr Opin Biotechnol 18:228–234
8. Bowden EF, Hawkridge FM, Blount HN (1985) Electrochemical aspects of bioenergetics. In: Srinivasan S, Chizmadzhev YA, Bockris JOM, Conway BE, Yeager E (eds) Comprehensive treatise of electrochemistry, vol 10. Plenum, New York, pp 297–346
9. Armstrong FA (1990) Probing metalloproteins by voltammetry. In: Bioinorganic chemistry, vol 72, Structure and bonding. Springer, Berlin, pp 137–221
10. Sarma AK, Vatsyayan P, Goswami P, Minteer SD (2009) Recent advances in material science for developing enzyme electrodes. Biosens Bioelectron 24:2313–2322
11. Prabhulkar S, Tian H, Wang X, Zhu J-J, Li C-Z (2012) Engineered proteins: redox properties and their applications. Antioxid Redox Signal 17:1796–1822
12. Hill HAO, Moore CB, NabiRahni DMA (1997) Electrochemistry of redox proteins. In: Lenaz G, Milazzot G (eds) Bioelectrochemistry of biomacromolecules. Birkhauser, Basel
13. Armstrong FA, Wilson GS (2000) Recent developments in faradaic bioelectrochemistry. Electrochim Acta 45:2623–2645
14. Habermüller K, Mosbach M, Schumann W (2000) Electron-transfer mechanisms in amperometric biosensors. Fresenius J Anal Chem 366:560–568
15. Ferapontova EE, Shleev S, Ruzgas T, Stoica L, Christenson A, Tkac J, Yaropolov AI, Gorton L (2005) Direct electrochemistry of proteins and enzymes. Perspectives in bioanalysis 1:517–598
16. Rusling JF, Wang B, Yun S (2008) Electrochemistry of redox enzymes. In: Bartlett PN (ed) Bioelectrochemistry, fundamentals, experimental techniques and applications. Wiley, Hoboken
17. Willner I, Katz E (eds) (2005) Bioelectronics from theory to applications. Wiley, Weinheim
18. Zhang W, Li G (2004) Third-generation biosensors based on the direct electron transfer of proteins. Anal Sci 20:603–609
19. Roger M, de Poulpiquet A, Ciaccafava A, Ilbert M, Guiral M, Giudici-Orticoni MT, Lojou E (2014) Reconstitution of supramolecular organization involved in energy metabolism at electrochemical interfaces for biosensing and bioenergy production. Anal Bioanal Chem 406:1011–1027
20. Léger C (2012) Direct electrochemistry of proteins and enzymes: an introduction
21. Laviron E (1979) General expression of the linear potential sweep voltammogram in the case of diffusionless electrochemical systems. J Electroanal Chem 101:19–28
22. Lisdat F, Schäfer D (2008) The use of electrochemical impedance spectroscopy for biosensing. Anal Bioanal Chem 391:1555–1567
23. Szamocki R, Velichko A, Mücklich F, Reculusa S, Ravaine S, Neugebauer S, Schuhmann W, Hempelmann R, Kuhn A (2007) Improved enzyme immobilization for enhanced bioelectrocatalytic activity of porous electrodes. Electrochem Commun 9:2121–2127
24. Patolsky F, Weizmann Y, Willner I (2004) Long-range electrical contacting of redox enzymes by SWCNT connectors. Angew Chem Int Ed 43:2113–2117
25. Yang J, Xu Y, Zhang R, Wang Y, He P, Fang Y (2009) Direct electrochemistry and electrocatalysis of the hemoglobin immobilized on diazonium-functionalized aligned carbon nanotubes electrode. Electroanalysis 21:1672–1677

26. Udit AK, Hagen KD, Goldman PJ, Star A, Gillan JM, Gray HB, Hill MG (2006) Spectroscopy and electrochemistry of cytochrome p450 BM3-surfactant film assemblies. J Am Chem Soc 128:10320–10325
27. Hagen KD, Gillan JM, Im S-C, Landefeld S, Mead G, Hiley M, Waskell LA, Hill MG, Udit AK (2013) Electrochemistry of mammalian cytochrome P450 2B4 indicates tunable thermodynamic parameters in surfactant films. J Inorg Biochem 129:30–34
28. Lioubashevski O, Chegel VI, Patolsky F, Katz E, Willner I (2004) Enzyme-catalyzed bio-pumping of electrons into Au-nanoparticles: a surface plasmon resonance and electrochemical study. J Am Chem Soc 126:7133–7143
29. Mateo C, Palomo JM, Fernandez-Lorente G, Guisan JM, Fernandez-Lafuente R (2007) Improvement of enzyme activity, stability and selectivity via immobilization techniques. Enzyme Microb Technol 40:1451–1463
30. Kotyk A, Janacek K, Koryta J (1988) Biophysical chemistry of membrane function. Wiley, Chichester
31. Jeuken LJC (2009) Electrodes for integral membrane enzymes. Nat Prod Rep 26:1234–1240
32. Melin F, Hellwig P (2013) Recent advances in the electrochemistry and spectroelectrochemistry of membrane proteins. Biol Chem 394:593–609
33. Rusling JF (1998) Enzyme bioelectrochemistry in cast biomembrane-like films. Acc Chem Res 31:363–369
34. Khan MS, Dosoky NS, Williams JD (2013) Engineering lipid bilayer membranes for protein studies. Int J Mol Sci 14:21561–21597
35. Jeuken LJC, Connell SD, Henderson PJF, Gennis RB, Evans SD, Bushby RJ (2006) Redox enzymes in tethered membranes. J Am Chem Soc 128:1711–1716
36. Beilen JB, Funhoff EG (2005) Expanding the alkane oxygenase toolbox: new enzymes and applications. Curr Opin Biotechnol 16:308–314
37. Udit AK, Gray HB (2005) Electrochemistry of heme-thiolate proteins. Biochem Biophys Res Commun 338:470–476
38. Walcarius A, Kuhn A (2008) Ordered porous thin films in electrochemical analysis. Trends Anal Chem 27:593–603
39. Szamocki R, Reculusa S, Ravaine S, Bartlett PN, Kuhn A, Hempelmann R (2006) Tailored mesostructuring and biofunctionalization of gold for increased electroactivity. Angew Chem Int Ed Engl 45:1317–1321
40. Wang CH, Yang C, Song YY, Gao W, Xia XH (2005) Adsorption and direct electron transfer from hemoglobin into a three-dimensionally ordered macroporous gold film. Adv Funct Mater 15:1267–1275
41. Rusling JF, Forster RJ (2003) Electrochemical catalysis with redox polymer and polyion–protein films. J Colloid Interface Sci 262:1–15
42. Vatsyayan P, Bordoloi S, Goswami P (2010) Large catalase based bioelectrode for biosensor application. Biophys Chem 153:36–42
43. Marcus RA, Sutin N (1985) Electron transfers in chemistry and biology. Biochim Biophys Acta 811:265–322
44. Henstridge MC, Laborda E, Rees NV, Compton RG (2012) Marcus–Hush–Chidsey theory of electron transfer applied to voltammetry: a review. Electrochim Acta 84:12–20
45. Plumeré N, Rüdiger O, Oughli AA, Williams R, Vivekananthan J, Pöller S, Schuhmann W, Lubitz W (2014) A redox hydrogel protects hydrogenase from high-potential deactivation and oxygen damage. Nat Chem 6:822–827
46. Malhotra BD, Chaubey A, Singh SP (2006) Prospects of conducting polymers in biosensors. Anal Chim Acta 578:59–74
47. Ahuja T, Mir IA, Kumar D, Rajesh (2007) Biomolecular immobilization on conducting polymers for biosensing applications. Biomaterials 28:791–805
48. Rahman MA, Kumar P, Park D-S, Shim Y-B (2008) Electrochemical sensors based on organic conjugated polymers. Sensors 8:118–141

49. Willner B, Katz E, Willner I (2006) Electrical contacting of redox proteins by nanotechnological means. Curr Opin Biotechnol 17:589–596
50. Xiao Y, Patolsky F, Katz E, Hainfeld JF, Willner I (2003) Plugging into enzymes: nanowiring of redox enzymes by a gold nanoparticle. Science 299:1877–1881
51. Campàs M, Prieto-Simón B, Marty J-L (2009) A review of the use of genetically engineered enzymes in electrochemical biosensors. Semin Cell Dev Biol 20:3–9
52. Sadeghi SJ, Meharenna YT, Fantuzzi A, Valetti F, Gilardi G (2000) Engineering artificial redox chains by molecular "lego". Faraday Discuss 116:135–153
53. Wong TS, Schwaneberg U (2003) Protein engineering in bioelectrocatalysis. Curr Opin Biotechnol 14:590–596
54. Marshall NM, Garner DK, Wilson TD, Gao Y-G, Robinson H, Nilges MJ, Lu Y (2009) Rationally tuning the reduction potential of a single cupredoxin beyond the natural range. Nature 462:113–117
55. Kumar S, Chen CS, Waxman DJ, Halpert JR (2005) Directed evolution of mammalian cytochrome P450 2B1, mutations outside of the active site enhance the metabolism of several substrates, including the anticancer prodrugs cyclophosphamide and ifosfamide. J Biol Chem 280:19569–19575
56. Axarli I, Prigipaki A, Labrou NE (2005) Engineering the substrate specificity of cytochrome P450 CYP102A2 by directed evolution: production of an efficient enzyme for bioconversion of fine chemicals. Biomol Eng 22:81–88
57. Sarauli D, Riedel M, Wettstein C, Hahn R, Stib K, Wollenberger U, Leimkühler S, Schmuki P, Lisdat F (2012) Semimetallic $TiO_2$ nanotubes: new interfaces for bioelectrochemical enzymatic catalysis. J Mater Chem 22:4615–4618
58. Pradhan D, Niroui F, Leung KT (2010) High-performance, flexible enzymatic glucose biosensor based on ZnO nanowires supported on a gold-coated polyester substrate. ACS Appl Mater Interfaces 2:2409–2412
59. Wanekaya AK, Chen W, Myung NV, Mulchandani A (2006) Nanowire-based electrochemical biosensors. Electroanalysis 18:533–550
60. Kumar AM, Jung S, Ji T (2011) Protein biosensors based on polymer nanowires, carbon nanotubes and zinc oxide nanorods. Sensors 11:5087–5111
61. Jacobs CB, Peairs MJ, Venton BJ (2010) Review: carbon nanotube based electrochemical sensors for biomolecules. Anal Chim Acta 662:105–127
62. Esplandiu MJ, Pacios M, Cyganek L, Bartroli J, del Valle M (2009) Enhancing the electrochemical response of myoglobin with carbon nanotube electrodes. Nanotechnology 20:355502
63. Cusmà A, Curulli A, Zane D, Kaciulis S, Padeletti G (2007) Feasibility of enzyme biosensors based on gold nanowires. Mater Sci Eng C 27:1158–1161
64. Dawson K, Baudequin M, O'Riordan A (2011) Single on-chip gold nanowires for electrochemical biosensing of glucose. Analyst 136:4507–4513
65. Mayorga-Martinez CC, Guix M, Madrid RE, Merkoci A (2012) Bimetallic nanowires as electrocatalysts for nonenzymatic real-time impedancimetric detection of glucose. Chem Commun 48:1686–1688
66. Travas-Sejdic J, Aydemir N, Kannan B, Williams DE, Malmström J (2014) Intrinsically conducting polymer nanowires for biosensing. J Mater Chem B 2:4593–4609
67. Wang Z, Liu S, Wu P, Cai C (2009) Detection of glucose based on direct electron transfer reaction of glucose oxidase immobilized on highly ordered polyaniline nanotubes. Anal Chem 81:1638–1645
68. Pingarron JM, Yanez-Sedeno P, Gonzalez-Cortes A (2008) Gold nanoparticle-based electrochemical biosensors. Electrochim Acta 53:5848–5866
69. Melin F, Meyer T, Lankiang S, Choi SK, Gennis RB, Blanck C, Schmutz M, Hellwig P (2013) Direct electrochemistry of cytochrome bo3 oxidase at a series of gold nanoparticles-modified electrodes. Electrochem Commun 26:105–108

70. Yu D, Renedo OD, Blankert B, Sima V, Sandulescu R, Arcos J, Kauffmann J-M (2006) A peroxidase-based biosensor supported by nanoporous magnetic silica microparticles for acetaminophen biotransformation and inhibition studies. Electroanalysis 18:1637–1642
71. Nowicka AM, Kowalczyk A, Donten ML, Donten M, Bystrzejewski M, Stojek Z (2014) Carbon-encapsulated iron nanoparticles as ferromagnetic matrix for oxygen reduction in absence and presence of immobilized laccase. Electrochim Acta 126:115–121
72. Kainz QM, Fernandes S, Eichenseer CM, Besostri F, Koerner H, Mueller R, Reiser O (2014) Synthesis of functionalized, dispersible carbon-coated cobalt nanoparticles for potential biomedical applications. Faraday Discuss 175:27–40
73. Kuila T, Bose S, Khanra P, Mishra AK, Kim NH, Lee JH (2011) Recent advances in graphene-based biosensors. Biosens Bioelectron 26:4637–4648
74. Armstrong FA (2005) Recent developments in dynamic electrochemical studies of adsorbed enzymes and their active sites. Curr Opin Chem Biol 9:110–117
75. Honeychurch M, The direct electrochemistry of cytochrome P450. What are we actually measuring? m.honeychurch@uq.edu.au
76. Fourmond V, Sabaty M, Arnoux P, Bertrand P, Pignol D, Leger C (2010) Reassessing the strategies for trapping catalytic intermediates during nitrate reductase turnover. J Phys Chem B 114:3341–3347
77. Leroux F, Dementin S, Burlat B, Cournac L, Volbeda A, Champ S, Martin L, Guigliarelli B, Bertrand P, Fontecilla-Camps J, Rousset M (2008) Experimental approaches to kinetics of gas diffusion in hydrogenase. Proc Natl Acad Sci U S A 105:11188–11193
78. Almeida MG, Silveira CM, Guigliarelli B, Bertrand P, Moura JJG, Moura I, Leger C (2007) A needle in a haystack: the active site of the membrane-bound complex cytochrome c nitrite reductase. FEBS Lett 581:284–288
79. Lautier T, Ezanno P, Baffert C, Fourmond V, Cournac L, Fontecilla-Camps JC, Soucaille P, Bertrand P, Meynial-Salles I, Leger C (2011) The quest for a functional substrate access tunnel in FeFe hydrogenase. Faraday Discuss 148:385–407
80. Liebgott P-P, Leroux F, Burlat B, Dementin S, Baffert C, Lautier T, Fourmond V, Ceccaldi P, Cavazza C, Meynial-Salles I, Soucaille P, Fontecilla-Camps JC, Guigliarelli B, Bertrand P, Rousset M, Léger C (2010) Relating diffusion along the substrate tunnel and oxygen sensitivity in hydrogenase. Nat Chem Biol 6:63–70
81. Rodriguez-Mozaz S, Lopez de Alda MJ, Marco MP, Barcelo D (2005) Biosensors for environmental monitoring A global perspective. Talanta 65:291–297
82. Grieshaber D, MacKenzie R, Vörös J, Reimhult E (2008) Electrochemical biosensors – sensor principles and architectures. Sensors 8:1400–1458
83. Ronkainen NJ, Halsall HB, Heineman WR (2010) Electrochemical biosensors. Chem Soc Rev 39:1747–1763
84. Yoo E-H, Lee S-Y (2010) Glucose biosensors: an overview of use in clinical practice. Sensors 10:4558–4576
85. Vaddirajua S, Tomazos I, Burgess DJ, Jain FC, Papadimitrakopoulosa F (2010) Emerging synergy between nanotechnology and implantable biosensors: a review. Biosens Bioelectron 25:1553–1565
86. Sassolas A, Prieto-Simón B, Marty J-L (2012) Biosensors for pesticide detection: new trends. Am J Anal Chem 3:210–232
87. Arya SK, Datta M, Malhotra BD (2008) Recent advances in cholesterol biosensor. Biosens Bioelectron 23:1083–1100
88. Saxena U, Chakraborty M, Goswami P (2011) Covalent immobilization of cholesterol oxidase on self-assembled gold nanoparticles for highly sensitive amperometric detection of cholesterol in real samples. Biosens Bioelectron 26:3037–3043
89. Saxena U, Das AB (2016) Nanomaterials towards fabrication of cholesterol biosensors: key roles and design approaches. Biosens Bioelectron 75:196–205
90. Male KB, Hrapovic S, Santini JM, Luong JHT (2007) Biosensor for arsenite using arsenite oxidase and multiwalled carbon nanotube modified electrodes. Anal Chem 79:7831–7837

91. Spricigo R, Dronov R, Lisdat F, Leimkühler S, Scheller FW, Wollenberger U (2009) Electrocatalytic sulfite biosensor with human sulfite oxidase co-immobilized with cytochrome c in a polyelectrolyte-containing multilayer. Anal Bioanal Chem 393:225–233
92. Bullen RA, Arnot TC, Lakeman JB, Walsh FC (2006) Biofuel cells and their development. Biosens Bioelectron 21:2015–2045
93. Davis F, Higson SPJ (2007) Biofuel cells—recent advances and applications. Biosens Bioelectron 22:1224–1235
94. Ivanov I, Vidaković-Koch T, Sundmacher K (2010) Recent advances in enzymatic fuel cells: experiments and modelling. Energies 3:803–846
95. Meredith MT, Minteer SD (2012) Biofuel cells: enhanced enzymatic bioelectrocatalysis. Annu Rev Anal Chem 5:157–179
96. Rasmussen M, Abdellaoui S, Minteer SD (2016) Enzymatic biofuel cells: 30 years of critical advancements. Biosens Bioelectron 76:91–102
97. Hambourger M, Gervaldo M, Svedruzic D, King PW, Gust D, Ghirardi M, Moore AL, Moore TA (2008) [FeFe]-hydrogenase-catalyzed $H_2$ production in a photoelectrochemical biofuel cell. J Am Chem Soc 130:2015–2022
98. Habrioux A, Merle G, Servat K, Kokoh KB, Innocent C, Cretin M, Tingry S (2008) Concentric glucose/$O_2$ biofuel cell. J Electroanal Chem 622:97–102
99. Sokic-Lazic D, Minteer SD (2008) Citric acid cycle biomimic on a carbon electrode. Biosens Bioelectron 24:939–944
100. Arechederra RL, Minteer SD (2009) Complete oxidation of glycerol in an enzymatic biofuel cell. Fuel cells 9:63–69
101. Sokic-Lazic D, Minteer SD (2009) Pyruvate/air enzymatic biofuel cell capable of complete oxidation. Electrochem Solid-State Lett 12:26–28